Remote Sensing of Environment 114 (2010) 977–994

Contents lists available at ScienceDirect

Remote Sensing of Environment

journal homepage: www.elsevier.com/locate/rse

Monitoring canopy biophysical and biochemical parameters in ecosystem scale using satellite hyperspectral imagery: An application on a *Phlomis fruticosa* Mediterranean ecosystem using multiangular CHRIS/PROBA observations

Stavros Stagakis [a,*], Nikos Markos [a], Olga Sykioti [b], Aris Kyparissis [a]

[a] University of Ioannina, Department of Biological Applications and Technology, Laboratory of Botany, GR-451 10, Ioannina, Greece
[b] Institute for Space Applications and Remote Sensing, National Observatory of Athens, Metaxa and Vas. Pavlou str., GR-152 36 Penteli, Athens, Greece

ARTICLE INFO

Article history:
Received 17 July 2009
Received in revised form 11 December 2009
Accepted 12 December 2009

Keywords:
Hyperspectral
Chlorophyll
CHRIS/PROBA
Carotenoids
Spectral index
Multiangular
LAI
Reflectance
Phlomis fruticosa
Water potential

ABSTRACT

This study focuses on the potential of satellite hyperspectral imagery to monitor vegetation biophysical and biochemical characteristics through narrow-band indices and different viewing angles. Hyperspectral images of the CHRIS/PROBA sensor in imaging mode 1 (5 observation angles, 62 bands, 410–1005 nm) were acquired throughout a two-year period for a Mediterranean ecosystem fully covered by the semi-deciduous shrub *Phlomis fruticosa*. During each acquisition, coincident ecophysiological field measurements were conducted. Leaf area index (LAI), leaf biochemical content (chlorophyll a, chlorophyll b, carotenoids) and leaf water potential were measured. The hyperspectral images were corrected for coherent noises, cloud and atmosphere, in order to produce ground reflectance images. The reflectance spectrum of each image was used to calculate a variety of vegetation indices (VIs) that are already published in relevant literature. Additionally, all combinations of the 62 bands were used in order to calculate Normalized Difference Spectral Indices ($NDSI_{(x,y)}$) and Simple Subtraction Indices ($SSI_{(x,y)}$). The above indices along with raw reflectance and reflectance derivatives were examined for linear relationship with the ground-measured variables and the strongest relationships were determined. It is concluded that higher observation angles are better for the extraction of biochemical indices. The first derivative of the reflectance spectra proved to be very useful in the prediction of all measured variables. In many cases, complex and improved spectral indices that are proposed in the literature do not seem to be more accurate than simple NDSIs such as NDVI. Even traditional broadband NDVI is proved to be adequate in LAI prediction, while green bands seem also very useful. However, in biochemical estimation narrow bands are necessary. Indices that incorporate red, blue and IR bands, such as PSRI, SIPI and mNDVI presented good performance in chlorophyll estimation, while CRI did not show any relevance to carotenoids and WI was poorly correlated to water potential. Moreover, analyses indicated that it is very important to use a near red-edge band (701 nm) for effective chlorophyll index design. SSIs that incorporate 701 nm with 511 or 605 nm showed best performance in chlorophyll determination. For carotenoid estimation, a band on the edge of carotenoid absorption (511 nm) combined with a red band performed best, while a normalized index of two water absorption bands (945, 971 nm) proved to be an effective water index. Finally, the attempt to investigate stress conditions through pigment ratios resulted in the use of the band centred at 701 nm.

1. Introduction

Multispectral sensors dominated satellite remote sensing in the last three decades. Despite their few and wide spectral bands, they have been a valuable source of information for earth observing purposes. The latest and most significant breakthrough in passive optical remote sensing has been the development of hyperspectral sensors on satellite platforms (e.g. EO-1 Hyperion, CHRIS/PROBA) providing continuous narrow bands and high resolution in the visible and infrared spectral region. Various methods and analyses may be applied on hyperspectral data in order to retrieve or examine relationships with ecosystem variables. Among the common applications is the use of the whole reflectance spectrum in assimilation techniques incorporating radiative transfer models (Dawson et al., 1998; Jacquemoud et al., 1996). Another simpler and widely used application is to extract empirical relationships between vegetation indices from the reflectance spectra and field measured plant variables.

* Corresponding author.
E-mail address: sstagaki@cc.uoi.gr (S. Stagakis).

0034-4257/$ – see front matter © 2010 Elsevier Inc. All rights reserved.
doi:10.1016/j.rse.2009.12.006

Several optical indices have arisen by relating leaf biochemical constituent concentrations with hyperspectral data. Many studies have focused on the investigation of effective hyperspectral chlorophyll indices (Carter, 1994; Gitelson and Merzlyak, 1997; Vogelmann et al., 1993; Zarco-Tejada et al., 2001, 2005), while carotenoids (Gitelson et al., 2002; Sims and Gamon, 2002) and water content (Peñuelas et al., 1993) have also been examined. Moreover, many recent studies that used hyperspectral data focused on improving the commonly and widely used Normalized Difference Vegetation Index (NDVI) and on developing new indices aiming to compensate for soil background influences (Bannari et al., 1996; Qi et al., 1994; Rondeaux et al., 1996), and atmospheric effects (Karnieli et al., 2001; Kaufman and Tanre, 1992).

Canopy reflectance in the visible and near infrared is strongly dependent on both structural (i.e. amount of leaves per area, leaf orientation, canopy structure) and biochemical properties (i.e. chlorophylls, carotenoids) of the canopy (Jacquemoud et al., 1996; Zarco-Tejada et al., 2001). Thus it is very difficult, if not impossible, to design a vegetation index (VI) exclusively sensitive to one plant variable (Govaerts et al., 1999). Airborne or satellite reflectance signal may be additionally influenced by soil and understorey reflectance, illumination and atmospheric conditions and the sensor observation geometry.

The ESA's pushbroom Compact High Resolution Imaging Spectrometer (CHRIS) offers unique multiangular capabilities. Observations from different viewing angles comprise a source of additional and necessary information, since they provide a means to characterize the anisotropy of surface reflectance (Chen et al., 2003). Multiangular observations contain much more information than nadir alone and provide the possibility to test recently developed narrow band indices for their directional response. VIs are expected to suffer from directionality because of the reflectance anisotropy of different vegetation types, canopy structure, non-photosynthetic material, background contributions and shadowing (Kimes et al., 1985; Qi et al., 1995). The lack of directional testing is a limiting factor for the potential use of the VIs for consistent and accurate long-term monitoring of vegetation on ecosystem scale. Multiangular views contain also information on the structure of vegetated surfaces and the shaded parts of the canopy (Chen et al., 2003; Gao et al., 2003).

Finally, hyperspectral data give the possibility to apply analyses such as multiple linear regression, principal component regression, partial least squares regression, derivatives (Grossman et al., 1996; Takahashi et al., 2000) and also to explore mathematical combinations of the various narrow spectral bands in order to expand the list of the proposed conventional indices.

This paper aims to explore the performance of existing vegetation indices and carry out tests and analyses, using satellite hyperspectral/multiangular reflectance spectra and coincident field measurements. To that purpose, images from CHRIS/PROBA were acquired for a Mediterranean ecosystem for a two-year study period. Reflectance spectra, their derivatives, proposed indices in the literature and potential band combinations are tested for linear relationships with field measured plant variables in an attempt to reveal hyperspectral dynamics in estimation and discrimination of different ecosystem variables. Different observing angles are also compared to explore directionality and performance of indices depending on the acquisition geometry.

2. Methods

2.1. Study site

The site selected is a phryganic shrubland located at the western part of northern Greece (39° 10.13′ N, 20° 51.00′ E, 59 m above sea level), about 25 km from the west coast. It is a typical Mediterranean ecosystem covered with the semi-deciduous shrub *Phlomis fruticosa* (canopy height ~1.5 m). The site area is about 500 m^2, dense and almost homogenous. Among the shrubs there are few very sparse trees (*Pyrus amygdaliformis* and *Olea europea*) and the topography is very smooth (landscape is almost flat). When the shrubs (*Phlomis fruticosa*) are at full leaf expansion the ground is fully covered by their canopies. During the hot and dry summer period, leaf biomass of *Phlomis fruticosa* is drastically reduced, thus canopy gaps appear and parts of the ground are exposed. *Phlomis fruticosa* is selected as especially suitable for this study because it shows strong fluctuations in phenological, physiological and biochemical parameters, following the seasonal climatic variability (Kyparissis and Manetas, 1993; Kyparissis et al., 1995).

2.2. Field ecophysiological measurements

Field measurements were conducted only at the days of CHRIS acquisitions (Table 1) during local midday (CHRIS acquisitions varied around 11:00 to 12:00 local time, GMT +2) and only on *Phlomis fruticosa* shrubs.

Table 1
Zenith (Z) and Azimuth (A) angles of the sun and CHRIS/PROBA for all acquisitions over the study site. Shaded dates were not used in the analyses. Dark shading refers to images where the study area is not included within the field of view, images with cloud perturbations above the study area, or images that an amount of bands showed undetermined peculiar radiances and could not be used in the analyses. At dates 4/7/2006 and 11/11/2007 field measurements were not conducted.

	Date	Sun		+55 °		+36 °		0 °		-36 °		-55 °	
		Z	A	Z	A	Z	A	Z	A	Z	A	Z	A
1	4/7/2006	20 °	139.42 °	48.72 °	7.37 °	27.73 °	1.29 °	6.93 °	224.19 °	32.46 °	201.76 °	51.53 °	197.97 °
2	12/7/2006	22 °	136.55 °	48.41 °	18.06 °	27.66 °	24.13 °	7.98 °	141.15 °	32.61 °	180.80 °	51.57 °	186.42 °
3	2/9/2006	34 °	154.09 °	54.49 °	12.59 °	32.30 °	13.03 °	3.62 °	186.39 °	37.39 °	192.16 °	57.24 °	192.51 °
4	24/10/2006	52 °	167.41 °	48.47 °	8.55 °	27.39 °	3.91 °	5.66 °	223.20 °	32.19 °	199.82 °	51.37 °	196.82 °
5	6/12/2006	63 °	166.87 °	52.95 °	12.00 °	30.79 °	11.73 °	4.15 °	198.53 °	36.94 °	193.33 °	56.69 °	193.15 °
6	15/4/2007	33 °	149.19 °	54.38 °	13.61 °	32.18 °	15.30 °	4.10 °	163.78 °	37.10 °	189.96 °	56.86 °	191.32 °
7	29/5/2007	22 °	140.21 °	48.63 °	3.84 °	28.21 °	353.78 °	10.8 °	224.87 °	33.40 °	206.53 °	51.89 °	201.02 °
8	11/7/2007	23 °	131.77 °	53.01 °	12.89 °	30.99 °	13.71 °	3.85 °	179.97 °	36.62 °	191.51 °	56.47 °	192.15 °
9	24/8/2007	32 °	146.80 °	51.43 °	5.62 °	30.10 °	357.55 °	9.54 °	224.67 °	35.04 °	204.15 °	53.97 °	199.43 °
10	6/10/2007	47 °	158.35 °	49.56 °	15.27 °	28.34 °	18.72 °	5.00 °	148.11 °	33.33 °	186.63 °	52.92 °	189.56 °
11	15/10/2007	50 °	161.20 °	–	–	–	–	–	–	–	–	–	–
12	11/11/2007	58 °	166.45 °	55.81 °	356.09 °	37.29 °	340.73 °	23.40 °	315.09 °	41.85 °	214.65 °	58.75 °	207.23 °
13	19/11/2007	60 °	164.28 °	54.35 °	9.03 °	32.27 °	5.14 °	6.08 °	222.40 °	37.31 °	198.7 °	56.92 °	196.12 °
14	14/2/2008	57 °	152.08 °	53.24 °	14.93 °	31.43 °	18.10 °	5.30 °	149.26 °	36.61 °	187.09 °	56.45 °	189.77 °
15	16/6/2008	24 °	125.14 °	54.32 °	8.12 °	32.20 °	3.07 °	7.47 °	222.91 °	38.12 °	200.02 °	57.56 °	196.89 °
16	4/7/2008	24 °	126.01 °	54.03 °	0.34 °	33.96 °	347.51 °	16.85 °	315.02 °	38.18 °	210.79 °	56.24 °	203.96 °
17	17/8/2008	32 °	138.13 °	49.84 °	357.31 °	31.47 °	342.60 °	18.25 °	315.09 °	35.57 °	213.77 °	52.86 °	206.40 °

Leaf area index (LAI) – incorporating ecosystem structural or biophysical variability – was measured using an indirect method that is based on an inversion of the Beer–Lambert equation (Monsi and Saeki, 1953):

$$\mathrm{LAI} = -\frac{1}{k}\ln\frac{I}{I_0} \quad (1)$$

where k is the canopy extinction coefficient, I_0 the incident Photosynthetically Active Radiation (PAR) above canopy and I the PAR transmitted below canopy. AccuPAR LP-80 PAR/LAI Ceptometer (Decagon Devices, Inc., Pullman, Washington—USA) was used to measure PAR above and below canopy. Extinction coefficient k is a function of leaf angle distribution, leaf azimuth angle (Jones, 1992) and the zenith angle of the sun (Campbell, 1986). Nevertheless, when all measurements of LAI are performed at constant time of the day (e.g. at local noon), in the same site and only at days with clear sky, it is often proposed that a constant k value could be used (Bréda, 2003). Combining the above method of determining LAI with the method that is proposed by Norman and Jarvis (1974), which is also used by the AccuPAR software, it was concluded that a constant value of $k=0.65$ should be used in Eq. (1) for the calculation of LAI. LAI measurements were organized by marking 10 individual shrubs in an area of about 125 m^2 and measuring LAI of each individual based on the above method. The average of the 10 individuals was considered indicative of the site, since the area is homogenous.

Leaf pigment concentration, i.e. chlorophyll a (CHLa), chlorophyll b (CHLb) and carotenoids (CAR), was measured spectrophotometrically in the laboratory, in 80% acetone extracts according to Lichtenthaler and Wellburn (1983), using a spectrophotometer (Hitachi U-2800, Tokyo, Japan). An amount of 60 leaves from the upper part of the canopy were randomly sampled from all the site area, sealed in plastic bags, placed in a dark, cool and dry box, transferred to the lab and measured immediately.

Leaf water potential (Ψ) was measured using a Scholander-type pressure chamber (SKPM 1400, Skye Instruments Ltd., UK). About 8 to 10 samples from the upper part of the canopy and randomly distributed along the site were wrapped in aluminum foil and sealed in plastic bags for 10 min and then cut and measured immediately with the pressure chamber.

2.3. CHRIS satellite data processing

The Compact High Resolution Imaging Spectrometer (CHRIS) of the ESA's Project for On Board Autonomy (PROBA) platform provides high spectral and spatial resolution hyperspectral/multiangular data. It acquires five consecutive images from five different observation angles (+55°, +36°, 0°, −36°, −55°) in one single satellite overpass. Negative observation angles correspond to acquisitions that the satellite has flown over the target position (Fig. 1). The negative observation angles may also be referred as backward scattering directions and the positive as forward scattering directions. The backward scattering observations can be defined as the acquisitions where the relative azimuth angle (difference between sensor and solar azimuth angle) is less or equal to 60° (Drolet et al., 2005). CHRIS can operate in different imaging modes reflecting a necessary compromise between spatial resolution and the number of spectral channels. In this study, CHRIS Mode 1, providing full spectral information (62 bands) with a spatial resolution of 34 m at nadir (at 556 km sensor altitude) was used. CHRIS mode 1 bands focus over the visible/near-infrared from 410 to 1005 nm, with spectral sampling interval ranging from 6 to 20 nm. The dates of the acquisitions planned for the study site were carefully selected so that the sensor zenith observation angle would be very near to zero degrees (Table 1).

It must be also noted that some acquisitions (especially those of −55° observation angle) failed to include the study area within the sensor's field of view (Table 1). Moreover, small shifts in CHRIS band wavelengths appeared in each acquisition. These shifts alter the minimum/maximum wavelength and the bandwidth of each band. Comparing with the prototype bands, as referred in the CHRIS data format issue, the discrepancy between the bands increases with the wavelength and band number. To be more accurate, regarding our analysis and index calculation, the actual band wavelengths of each acquisition were extracted from the image metadata. Then, the central wavelengths and the bandwidths of all images were averaged and the analysis was based upon these actual central wavelengths and bandwidths.

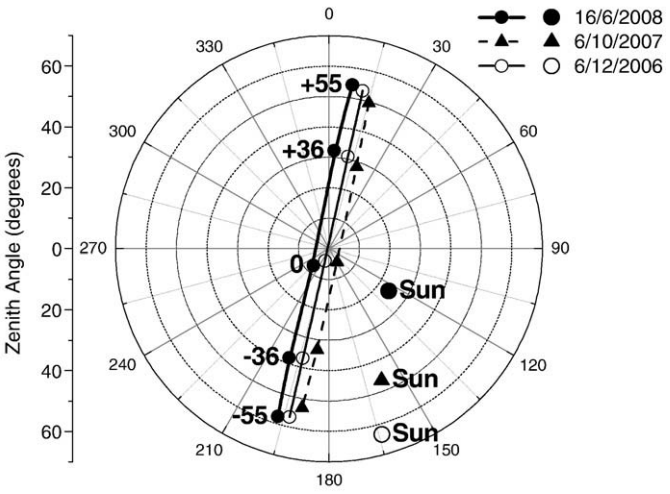

Fig. 1. Polar plot of three typical acquisition and illumination geometries of CHRIS/PROBA over the study site. The negative observation angles (−36, −55) correspond to backward scattering directions and the positive (+36, +55) to forward scattering directions.

CHRIS data were (pre)processed using CHRIS-Box software developed as extension for the BEAM tool (Brockmann Consult, http://www.brockmann-consult.de/beam). Drop-outs and vertical striping were corrected or reduced before any further processing, using the algorithm of Gómez-Chova et al. (2008). At the next step, cloud screening was performed so that all cloudy pixels would be identified and masked. After noise reduction and cloud masking, the images were atmospherically corrected according to the method described by Guanter et al. (2006). Each final image consists of a surface reflectance image with cloud mask and columnar water vapor (CWV) map.

The study area was determined after geolocation of the images using GPS determined ground control points (GCPs). Reflectance spectra of the site area were extracted using an average of 8 pixels at the observation angles −36°, 0°, +36° and 6 pixels at the observation angles −55°, +55°. These final reflectance curves still presented noise, seen as rapid and random changes in amplitude from point to point within the signal. These slight abnormalities were eliminated performing a 3-point fast Fourier transform (FFT) algorithm on the reflectance curves. A systematic error was found in the first band (centred at 411 nm) appearing extreme low (even negative) values, especially in the forward scattering viewing angles.

2.4. Spectral analysis and indices calculation

Each observation angle was processed as an individual set of reflectance measurements and the following analysis was applied separately for the different observation angle sets. Observation angle −55° was excluded from the analysis since it is absent from a significant number of acquisitions (Table 1).

Several indices and index types were developed, examined and compared based on their linear relationship with every field

measured plant variable, in order to discover which index is best for the prediction of each variable. The amount of green biomass that the studied ecosystem develops does not reach high levels where VIs tend to saturate (Wang et al., 2005), consequently the use of non-linear relationships would not offer significant advantage over linear ones in the present study. The comparison of the indices was based upon the

Table 2
Narrowband and broadband indices, proposed in relevant literature, that are tested in the present study. Indices are sorted according to their original design and expected function.

Index	Formulation	Reference
Broadband Greenness		
EVI *(Enhanced Vegetation Index)*	$2.5\frac{R_{nir}-R_{red}}{R_{nir}+6R_{red}-7.5R_{blue}+1}$	Huete et al. (1997)
Green NDVI *(green Normalized Difference Vegetation Index)*	$(R_{nir}-R_{green})/(R_{nir}+R_{green})$	Gitelson et al. (1996)
NDVI *(Normalized Difference Vegetation Index)*	$(R_{nir}-R_{red})/(R_{nir}+R_{red})$	Tucker (1979)
SR *(Simple Ratio)*	R_{nir}/R_{red}	Jordan (1969)
Narrowband Greenness		
CARI *(Chlorophyll Absorption Ratio Index)*	$\frac{R_{700}\lvert a670+R_{670}+b\rvert}{R_{670}(a^2+1)^{0.5}}, a=\frac{R_{700}-R_{550}}{150}, b=R_{550}-a550$	Kim et al. (1994)
GI *(Greenness Index)*	R_{554}/R_{677}	Zarco-Tejada et al. (2005)
GVI	$(R_{682}-R_{553})/(R_{682}+R_{553})$	Gandia et al. (2004)
mCAI *(modified Chlorophyll Absorptions Integral)*	$A-\int_{R552}^{R752}f$, A = area of the trapeze between R_{752} and R_{552}, f = reflectance curve	Oppelt and Mauser (2001)
mCAI2 *(modified Chlorophyll Absorptions Integral)*	$A-\int_{R600}^{R735}f$, A = area of the trapeze between R_{735} and R_{600}, f = reflectance curve	Oppelt and Mauser (2001)
MCARI *(Modified Chlorophyll Absorption Ratio Index)*	$[(R_{700}-R_{670})-0.2(R_{700}-R_{550})](R_{700}/R_{670})$	Daughtry et al. (2000)
MCARI2 *(Modified Chlorophyll Absorption Ratio Index)*	$1.2[2.5(R_{800}-R_{670})-1.3(R_{800}-R_{550})]$	Haboudane et al. (2004)
mNDVI *(Modified Normalized Difference Vegetation Index)*	$(R_{800}-R_{680})/(R_{800}+R_{680}-2R_{445})$	Sims and Gamon (2002)
mNDVI2 *(Modified Normalized Difference Vegetation Index)*	$(R_{750}-R_{705})/(R_{750}+R_{705}-2R_{445})$	Sims and Gamon (2002)
MSAVI *(Improved Soil Adjusted Vegetation Index)*	$0.5[2R_{800}+1-\sqrt{(2R_{800}+1)^2-8(R_{800}-R_{670})}]$	Qi et al. (1994)
mSR *(Modified Simple Ratio)*	$(R_{800}-R_{445})/(R_{680}-R_{445})$	Sims and Gamon (2002)
mSR2 *(Modified Simple Ratio)*	$(R_{750}-R_{445})/(R_{705}-R_{445})$	Sims and Gamon (2002)
MTCI *(MERIS Terrestrial Chlorophyll index)*	$(R_{754}-R_{709})/(R_{709}-R_{681})$	Dash and Curran (2004)
mTVI *(modified Triangular Vegetation Index)*	$1.2[1.2(R_{800}-R_{550})-2.5(R_{670}-R_{550})]$	Haboudane et al. (2004)
NDVI *(Normalized Difference Vegetation Index)*	$(R_{800}-R_{670})/(R_{800}+R_{670})$	Tucker (1979)
NDVI2 *(Normalized Difference Vegetation Index)*	$(R_{750}-R_{705})/(R_{750}+R_{705})$	Gitelson and Merzlyak (1994)
OSAVI *(Optimized Soil-Adjusted Vegetation Index)*	$1.16(R_{800}-R_{670})/(R_{800}+R_{670}+0.16)$	Rondeaux et al. (1996)
RDVI *(Renormalized Difference Vegetation Index)*	$(R_{800}-R_{670})/\sqrt{(R_{800}+R_{670})}$	Roujean and Breon (1995)
REP *(Red-Edge Position)*	$700+40\frac{[(R_{670}+R_{780})/2]-R_{700}}{R_{740}-R_{700}}$	Guyot et al. (1988)
SIPI *(Structure Insensitive Pigment Index)*	$(R_{800}-R_{450})/(R_{800}-R_{650})$	Peñuelas et al. (1995)
SIPI2	$(R_{800}-R_{440})/(R_{800}-R_{680})$	Peñuelas et al. (1995)
SPVI *(Spectral polygon vegetation index)*	$0.4[3.7(R_{800}-R_{670})-1.2\lvert R_{530}-R_{670}\rvert]$	Vincini et al. (2006)
SR *(Simple Ratio)*	R_{800}/R_{680}	Jordan (1969)
SR1, SR2, SR3	R_{750}/R_{700} R_{752}/R_{690} R_{750}/R_{550}	Gitelson and Merzlyak (1997)
SR4	R_{672}/R_{550}	Datt (1998)
TCARI *(Transformed Chlorophyll Absorption Ratio Index)*	$3[(R_{700}-R_{670})-0.2(R_{700}-R_{550})(R_{700}/R_{670})]$	Haboudane et al. (2002)
TSAVI *(Transformed Soil-Adjusted Vegetation Index)*	$a(R_{875}-aR_{680}-b)/[R_{680}+a(R_{875}-b)+0.08(1+a^2)]$, $\alpha=1.062$, $b=0.022$	Rondeaux et al. (1996)
TVI *(Triangular Vegetation Index)*	$0.5[120(R_{750}-R_{550})-200(R_{670}-R_{550})]$	Broge and Leblanc (2001)
VOG *(Vogelmann Indices)*	R_{740}/R_{720}	Vogelmann et al. (1993)
VOG2	$(R_{734}-R_{747})/(R_{715}+R_{726})$	Zarco-Tejada et al. (2001)
Leaf pigment (Carotenoids, Anthocyanins)		
ARI *(Anthocyanin Reflectance Index)*	$(1/R_{550})-(1/R_{700})$	Gitelson et al. (2001)
BGI *(Blue Green Pigment Index)*	R_{450}/R_{550}	Zarco-Tejada et al. (2005)
BRI *(Blue Red Pigment Index)*	R_{450}/R_{690}	Zarco-Tejada et al. (2005)
CRI *(Carotenoid Reflectance Index)*	$(1/R_{510})-(1/R_{550})$	Gitelson et al. (2002)
CRI2	$(1/R_{510})-(1/R_{700})$	Gitelson et al. (2002)
Red/Green	R_{red}/R_{green}	Gamon and Surfus (1999)
RGI *(Red/Green)*	R_{690}/R_{550}	Zarco-Tejada et al. (2005)
Stress		
CI *(Curvature Index)*	$R_{675}R_{690}/R_{683}^2$	Zarco-Tejada et al. (2003)
DI *(Derivative Index)*	D_{730}/D_{706}	Zarco-Tejada et al. (2003)
DPR2	D_{REP}/D_{725}	Zarco-Tejada et al. (2003)
DREP *(Derivative on the Red-Edge Position)*	D_{REP}	Horler et al. (1983)
LIC	R_{440}/R_{690}	Lichtenthaler et al. (1996)
NPCI *(Normalized Pigment Chlorophyll index)*	$(R_{680}-R_{430})/(R_{680}+R_{430})$	Peñuelas et al. (1994)
NPQI *(Normalized Phaeophytinization Index)*	$(R_{415}-R_{435})/(R_{415}+R_{435})$	Barnes et al. (1992)
PRI *(Photochemical Reflectance Index)*	$(R_{531}-R_{570})/(R_{531}+R_{570})$	Gamon et al. (1997)
PRI2	$(R_{570}-R_{539})/(R_{570}+R_{539})$	Filella et al. (1996)
PSRI *(Plant Senescence Reflectance Index)*	$(R_{680}-R_{500})/R_{750}$	Merzlyak et al. (1999)
SR5, SR6	R_{690}/R_{655} R_{685}/R_{655}	Zarco-Tejada et al. (2003)
SRPI *(Simple Ratio Pigment Index)*	R_{430}/R_{680}	Peñuelas et al. (1995)
Water		
fWBI *(floating Water Band Index)*	$R_{900}/\min R_{920-980}$	Peñuelas et al. (1993)
WI *(Water Index)*	R_{900}/R_{970}	Peñuelas et al. (1993)

R_x stands for reflectance at wavelength x nm.
D_x stands for the derivative of the reflectance spectrum at wavelength x nm.
red: 620–670 nm, *nir*: 840–880 nm, *blue*: 460–480 nm, *green*: 545–565 nm; according to MODIS spectral bands.

coefficients of determination (r^2) of each linear relationship. The analysis was categorised into five main sections based on the different index types:

1. The first and most simple index type (R_x) is the reflectance value (R) at the central wavelength (x nm) of each band.
2. The second index type, i.e. the reflectance first derivative of each band's central wavelength (D_x), was extracted after the differentiation of the reflectance spectrum.
3. A variety of already proposed vegetation indices that can be applied to hyperspectral imagery were retrieved from the relevant literature. Most of them are designed for application at the canopy scale and only a few at the leaf scale. Table 2 shows the formulas of the published indices that were used in this study. All of the published hyperspectral indices were adjusted to CHRIS bands, i.e. for each reflectance wavelength of the prototype formula (Table 2), the actual CHRIS band central wavelengths were compared and the band that was closest to each prototype formulation wavelength was used.
   The fourth and the fifth section consist of all possible combinations of the 62 CHRIS bands based on two general index formulas.
4. The most widely used formula of a vegetation index is the normalized difference formula:

$$NDSI_{(x,y)} = \frac{R_x - R_y}{R_x + R_y}. \quad (2)$$

   The Normalized Difference Spectral Indices (NDSIs) combine the reflectance (R) of two bands (x, y are the central wavelengths of each band) and are widely used for scientific and operational applications. The normalisation is useful for reducing atmospheric or other sources of disturbances, cancelling the proportional changes of the reflectance spectrum, as well as enhancing the spectral response to observed targets (Huete et al., 1985; Qi et al., 1994). In this study, all combinations of the 62 CHRIS bands were applied in the NDSI formula. It has to be noted that $NDSI_{(x,y)} = -NDSI_{(y,x)}$ and the range of NDSIs is from −1 to 1.
5. Except from the widely used NDSI formula, a formula that also includes two bands but lacks normalisation was examined. The formula is referred as simple subtraction formula:

$$SSI_{(x,y)} = R_x - R_y. \quad (3)$$

   Simple Subtraction Indices (SSIs) have been rarely used on satellite data. This kind of indices does not offer much in standardization of the spectral response like the normalized indices. The only improvements, comparing to R_x, is that they contain information of two bands and are insensitive to additive changes of the reflectance spectrum. It is obvious that $SSI_{(x,y)} = -SSI_{(y,x)}$.

In this study, vegetation indices (VIs) are also examined for their performance in different viewing angles. Therefore every index is defined by the band central wavelengths (x, y nm) used and the observing angle (Z°), as $VI_{(x,y)}Z°$.

3. Results

3.1. Field measurements and CHRIS spectra

In Fig. 2 the seasonal fluctuation of the field-measured plant variables across the two-year study period is presented. As expected, there were intense variations of all measured physiological parameters during the growing period (Kyparissis and Manetas, 1993; Kyparissis et al., 1995). A covariance is evident between these parameters, with minimum values appearing during summer, when high temperature and limited precipitation restrict plant growth, and maximum values appearing after the onset of the autumn rains and during winter and early spring. The autumn revival is different for each variable, with water potential and chlorophyll content showing very quick responses, while carotenoids and LAI showing slower responses. Low winter temperature may also affect chlorophyll content, since a slight decline is observed during December to February, whereas carotenoids seem to preserve high concentrations, probably protecting chlorophylls against photooxidative stress.

In Fig. 3 the reflectance spectra of two extreme ecosystem phases are presented, i.e. under spring favorable conditions (April) and during the summer stress period (August), when plants are in an almost leafless and dry phase. The difference is obvious in the reflectance spectra that appear similar to the typical green leaf spectrum in spring and to an almost typical dry ground profile in August. It is also evident that observation angle −36° shows the greatest reflectance values followed by the nadir looking and the forward scattering observations. The discrepancies of reflectance spectra between the viewing directions are due to combinations of canopy gaps and backshadow effects (Deering et al., 1999; Sandmeier et al., 1998).

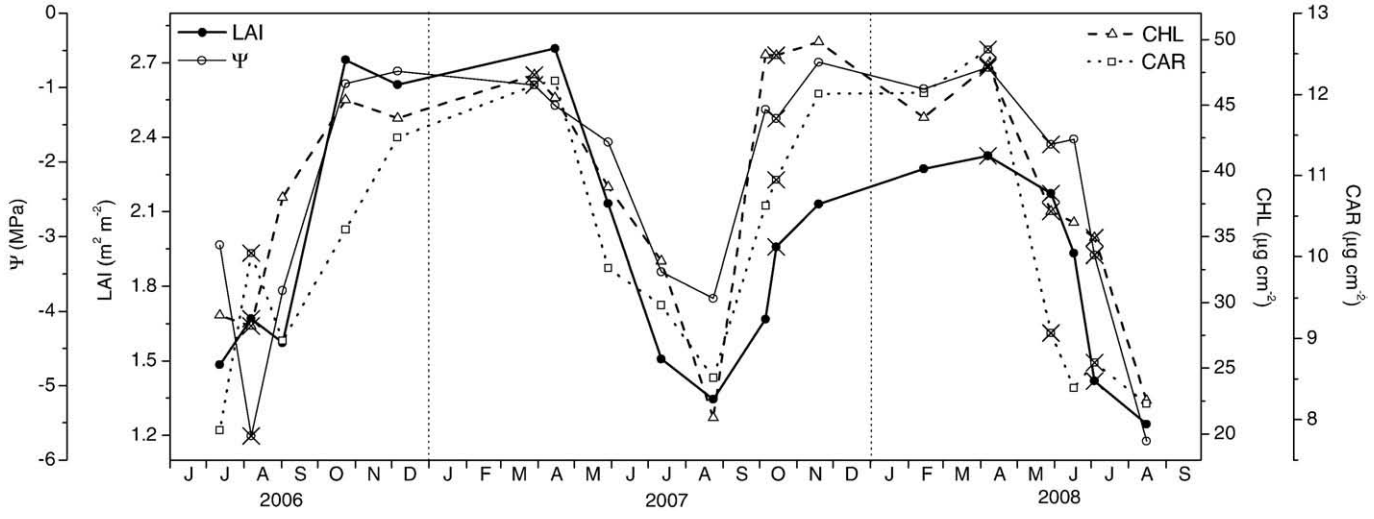

Fig. 2. Seasonal fluctuation of the field-measured variables: Leaf Area Index (LAI), chlorophyll content (CHL), carotenoid content (CAR) and Water Potential (Ψ). X over symbols denotes dates without CHRIS acquisitions or with acquisition and images not suitable for analysis (see also Table 1).

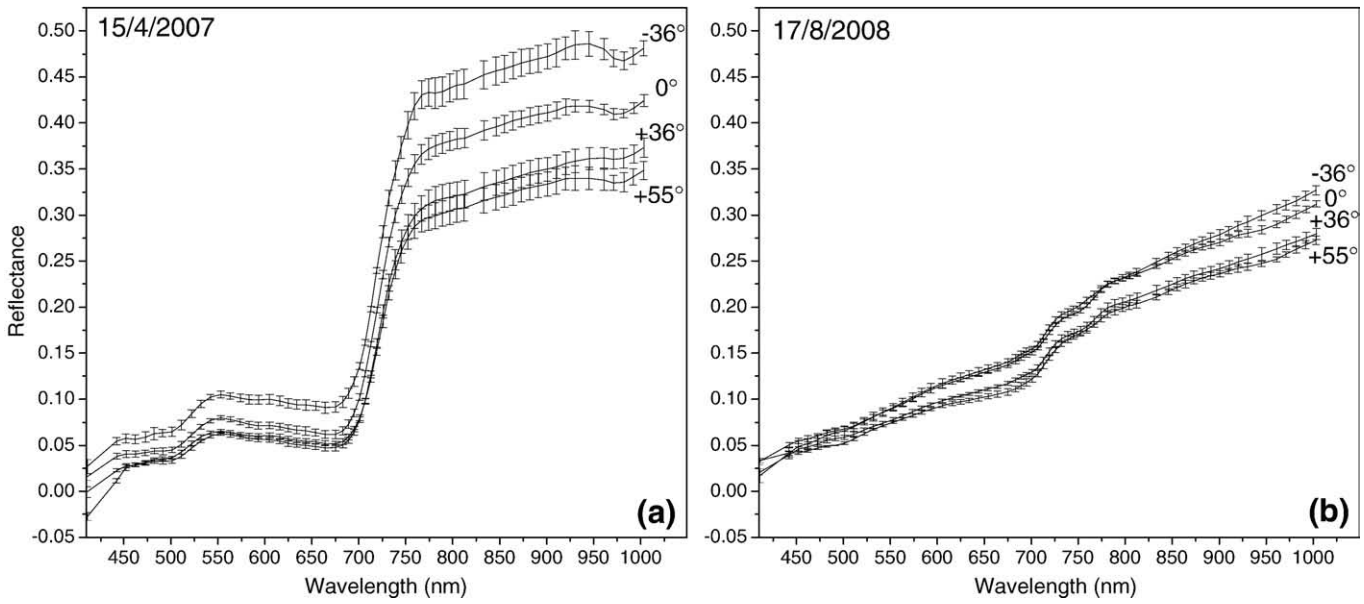

Fig. 3. Average and standard deviation of study site reflectance spectra for the four used CHRIS observation angles on 15/4/2007 and 17/8/2008.

3.2. Relationship of ecophysiological variables with reflectance spectra

The tests of the linear relationships between band reflectance and the measured ecosystem attributes showed various good coefficients of determination (r^2), revealing also the differentiation of the optimal bands according to the viewing angle. Generally, the yellow to red region of the visible part of the spectrum is the most useful for the estimation of the measured biophysical and biochemical parameters (Fig. 4). Many of the variables show best correlations with red and red-edge bands between 675 and 713 nm (Table 3), while near infrared (NIR) bands (mainly 745–767 nm and 930–945 nm) also show relatively good correlations with most of the variables.

LAI gets higher coefficients from the zenith and +36° viewing angles (Fig. 4a) in red wavelengths, with peak at 675 nm, near the band of chlorophyll maximum absorbance. As for the rest of the variables, it is evident that the +55° observing angle shows the highest coefficients (Fig. 4b–f). This is more pronounced in chlorophyll determination where bands between 689 and 701 nm show the highest coefficients for CHLa (Table 3), whereas a peak at 707 nm in the +55° angle distinguishes CHLb from the rest of the measured parameters (Fig. 4d). It is interesting to note that only the +55° angle shows high coefficients for CHLb determination.

CAR show high coefficients of determination with the red bands but also with NIR bands (Fig. 4c), with the most significant r^2 at 739 nm (Table 3). Ψ also shows best coefficients at the +55° observing angle and at 675 nm (Fig. 4e), probably due to its covariance with pigment concentration.

Lastly, CHL/CAR was examined, as it may express an insight in plant physiology, since its seasonal fluctuations reflect modifications of the photosynthetic machinery either towards photoselection or photoprotection (Balaguer et al., 2002; Kyparissis et al., 1995, 2000; Munné-Bosch and Alegre, 2000). It is shown that the +55° angle serves best in the determination of this ratio (Fig. 4f) and high coefficients are found between 583 and 707 nm with a peak between 701 and 707 nm. It is interesting noting that these spectral areas are correlated also with CHLa and CHLb in the same observation angle.

It is also worth to note that the reflectance at 719 nm, right in the middle of the red-edge, shows no relationship with any variable in the forward scattered and zenith directions. Moreover, the only backward scattering observing direction that is available (−36°) presents different significance pattern compared to the forward scattering and zenith directions, with lower coefficients in the visible part of the spectrum and increased coefficients in the IR part. Finally, the significance curves of −36° decrease earlier than the other angles after the usual peak in the visible (675–689 nm), reach zero in lower wavelengths (707 nm) and then increase earlier in the IR.

3.3. Relationship of ecophysiological variables with reflectance spectra derivatives

The first derivative of the reflectance spectrum appears to be more useful than raw reflectance values for the estimation of plant variables, since it revealed far more significant relationships with all of the measured parameters (Table 3). The derivative of the yellow to red region appears to correlate very well with most of the plant variables (Fig. 5), while among the observing angles, +55° shows the best coefficients. Comparing the curves between the variables two significance patterns may be distinguished. LAI, CHLa, CAR and Ψ (Fig. 5a–c,e) show high correlation in all observation angles with reflectance derivatives between 553 and 732 nm and between 930 and 971 nm, with a distinct low correlation area at 675–689 nm. On the other hand, for CHLb and CHL/CAR (Fig. 5d,f), observing angle +55° stands out among the four studied angles, while the derivatives at 473 nm, 542 nm, 675 nm, 920 nm and 971 nm show high significance for the determination of both variables.

The most interesting derivatives in chlorophyll determination are in the green (D_{553}) and red (D_{675}) part of the spectrum, both in the +55° observing angle (Table 3). D_{411} and D_{511} in the −36° observing angle seem suitable for CAR estimation, since they show high r^2 for CAR and low for LAI and chlorophylls (Fig. 5). Concerning CHLb and CHL/CAR, even though only the +55° observing angle shows significant correlations, it is worth noting two peaks – at 542 and 675 nm – appearing in common for both parameters (Fig. 5d,f). Additionally, a high significance area appears between 833 and 855 for CHL/CAR, proposing D_{833} and D_{855} as possible plant stress indices (Fig. 5f).

3.4. Relationship of ecophysiological variables with published indices

As shown in Table 4, LAI correlates strongly with many published indices from all of the categories and in all observing angles. Among the greenness indices (broadband and narrowband), only MTCI shows no correlation with LAI in all observing angles. However, the improved indices (e.g. EVI, RDVI, mNDVI, mSR, MSAVI, OSAVI, TVI,

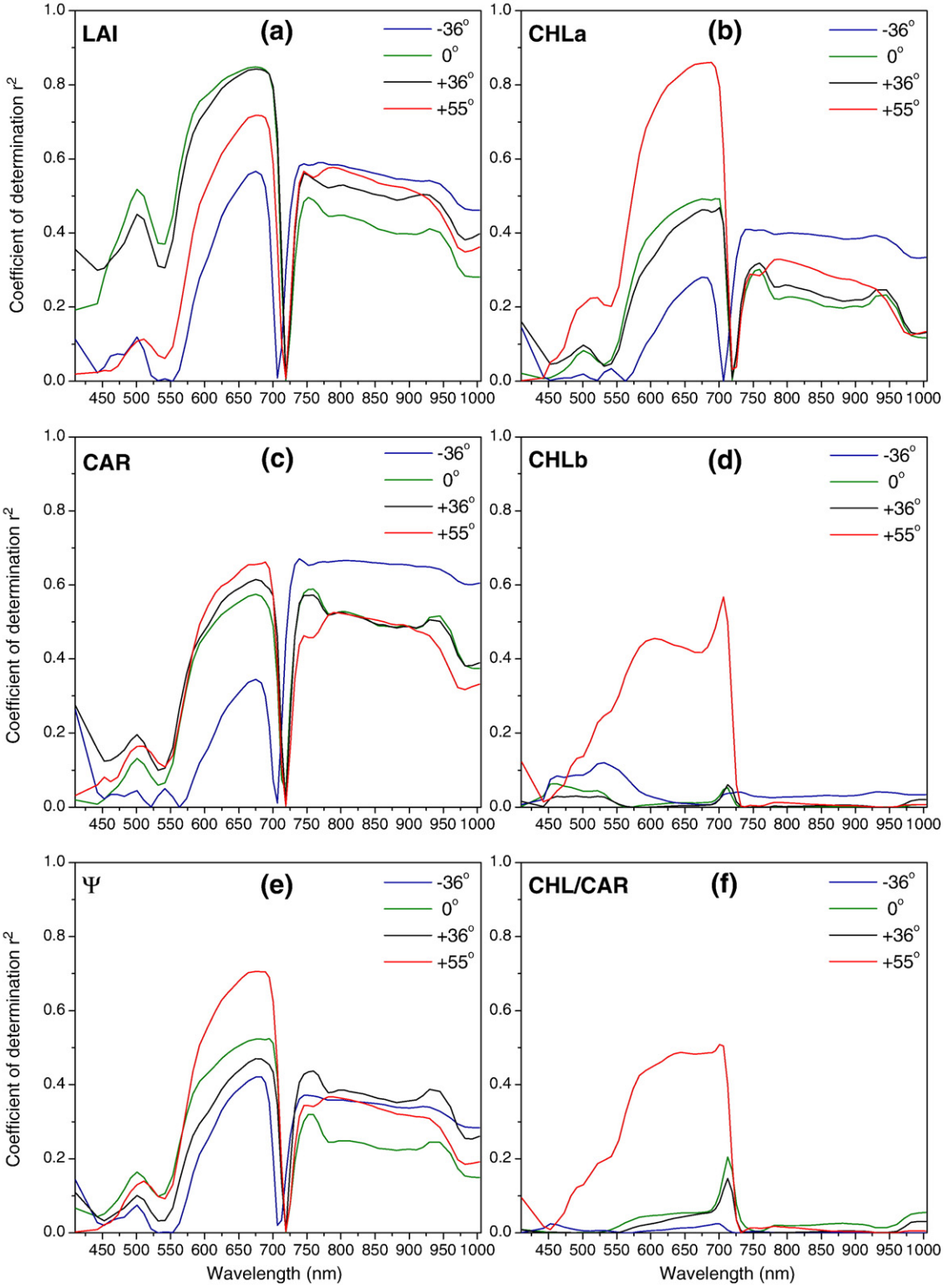

Fig. 4. Coefficients of determination (r^2) between CHRIS reflectance (R_x) and the ground measured biophysical and biochemical parameters for the four of the CHRIS observation angles.

SPVI) do not show any advantage over the traditional ones (broadband and narrowband NDVI and SR). It is important to note that the studied ecosystem does not reach high LAI values where traditional NDVI is believed to saturate. It is also interesting to note that LAI correlates better with indices that use bands in red and green than in red and NIR, such as GI, RGI and SR4, which show the maximum coefficients of determination for the forward scattering and zenith observing angles (Table 3). Another interesting point is that PRI, which is proposed to correlate with plant photoprotective responses (Gamon et al., 1997) and eventually with ecosystem function, shows very good covariance with LAI. In fact, the maximum r^2 for LAI in the backscattering direction is found with PRI2.

Contrasting with LAI, leaf chlorophyll content does not correlate well with many of the examined published indices (Table 4). CHLa

Table 3
Maximum coefficients of determination (r^2) between CHRIS band reflectance R_x, band reflectance derivatives D_x, published indices (Table 2) and the ground measured biophysical and biochemical parameters for the four of the CHRIS observation angles. x corresponds to either index wavelength (R_x, D_x) or published index abbreviation.

	+55°		+36°		0°		−36°	
	r^2	x	r^2	x	r^2	x	r^2	x
Band reflectance R_x								
LAI	0.718	675	0.843	675	0.849	675	0.591	767
CHLa	0.860	689	0.468	701	0.493	695	0.410	745
CHLb	0.567	707	0.061	713	0.063	462	0.121	532
CHL	0.856	689	0.410	701	0.436	701	0.369	739
CAR	0.661	689	0.615	675	0.589	759	0.671	739
CHL/CAR	0.508	701	0.147	713	0.205	713	0.025	701
Ψ	0.706	675	0.471	675	0.525	695	0.421	683
Derivative D_x								
LAI	0.923	654	0.905	593	0.891	616	0.877	563
CHLa	0.889	605	0.828	961	0.800	961	0.647	945
CHLb	0.589	675	0.541	971	0.506	920	0.335	910
CHL	0.865	553	0.818	961	0.770	961	0.589	945
CAR	0.817	945	0.812	616	0.799	574	0.766	511
CHL/CAR	0.702	855	0.547	971	0.366	920	0.304	873
Ψ	0.850	574	0.766	961	0.674	634	0.672	945
Indices								
LAI	0.909	GI	0.915	RGI	0.862	SR4	0.916	PRI2
CHLa	0.886	PSRI	0.679	TVI/OSAVI	0.733	PRI	0.673	PSRI
CHLb	0.609	CARI	0.558	MTCI	0.536	MTCI	0.473	DI
CHL	0.861	PSRI	0.616	PRI	0.684	PRI	0.636	DI
CAR	0.825	WI	0.821	PRI2	0.839	PRI2	0.780	GI
CHL/CAR	0.633	SIPI2	0.298	DPR2	0.268	DI	0.650	DPR2
Ψ	0.842	PSRI	0.802	TVI/OSAVI	0.779	REP	0.788	SIPI

shows significant correlations with some indices mostly in the +55° direction (e.g. mNDVI, PSRI and SIPI), although indices that use red and green bands also tend to correlate well. PSRI seems to be the best index for the estimation of leaf chlorophyll content, since it shows the maximum coefficients (+55° observing angle) in CHLa and total chlorophyll determination (Table 3). Most of the stress indices in Table 2 (e.g. PSRI, DREP) are designed to detect chlorophyll attributes related to plant health, thus it is reasonable to be correlated with chlorophyll concentration. The improved complex greenness indices that are proposed to detect chlorophyll variations (e.g. CARI, mCAI, MCARI, TCARI) do not seem to excel compared to simpler ones (e.g. NDVI); many of them do not even show significant relationships with leaf chlorophyll content in some observing angles.

CAR shows various significant correlations with many published indices from all of the categories and in all observing angles (Table 4). Most of them coincide with the indices that correlate with LAI and chlorophyll content. The best correlations are found with WI, PRI and PRI2 (Table 3). Given that both WI and PRI are designed to detect stress conditions in leaves and that carotenoid concentration is related to plant photoprotective mechanisms, the above result seems reasonable. Lastly, it is worth to note that CRI, an index designed for leaf carotenoid estimation, did not show any correlation with carotenoid content.

Indices WI and fWBI are the only indices used in this study that are designed for the detection of plant water content. They use the only available part of the spectrum (920–980 nm, water absorption) where water contamination may be visible. Unfortunately, WI presented low r^2 and fWBI did not present any significant relationship with Ψ, while the strongest correlations appear with almost the same indices as chlorophyll content (Table 4).

3.5. Analysis of the $NDSI_{(x,y)}$ formula experimental combinations

The 62 CHRIS bands were used in order to calculate and test all the possible indices of the $NDSI_{(x,y)}$ formula. Taken into account that $NDSI_{(x,y)} = -NDSI_{(y,x)}$, there are 1891 different combinations possible. All these NDSIs were tested for linear relationship with all measured variables and the coefficients of determination (r^2) between NDSIs and each variable were plotted in contour maps, providing an overview of the statistical significance of each NDSI band combination (Fig. 6). The optimal NDSIs vary for each ecosystem variable and among the observing angles. NDSIs of high significance are usually combinations of red (including red-edge) and IR wavelengths, red and green wavelengths and between IR wavelengths (focused mainly around the water absorption bands, 920–970 nm).

It is clear that there are many effective NDSIs for LAI estimation in all observation angles (Fig. 6a–d). There is a large region of high coefficients at NDSIs with x: ~580–720 nm and y: ~710–1003 nm evident in all observing angles except the backscattering angle −36°, where the above region is slightly smaller. There is another wide region of high significance in red–green NDSIs with x: ~510–650 nm and y: ~570–695 nm. In the backscatter direction the latter is a little wider including the part x: ~470–510 nm and y: ~640–690 nm. These two big regions indicate that LAI can be reliably estimated by broadband indices like the traditional NDVI. In fact, the first and wider region is by definition a broadband NDVI (Table 2). However, inside the red–green region there are some smaller areas of extremely high significance (r^2>0.9), varying among the different observing angles. The greater region of extreme high significance (r^2>0.9) appears in the +55° observing angle at NDSIs with x: ~530–640 nm and y: ~670–690 nm. These findings suggest that even though a broadband NDVI can be reliable for LAI estimation, narrow band indices at high observing angles can be more effective. Table 5 shows the NDSIs of highest r^2 for every variable tested. It is noticeable that NDSIs with x, y bands that are close to each other tend to reach maximum significance in LAI determination. It is also evident that in the backscattering direction the highest coefficients for LAI are focussed around the wavelengths of the PRI formula (Fig. 6d). It is important to note that in zenith observing angle (Fig. 6c) there are no

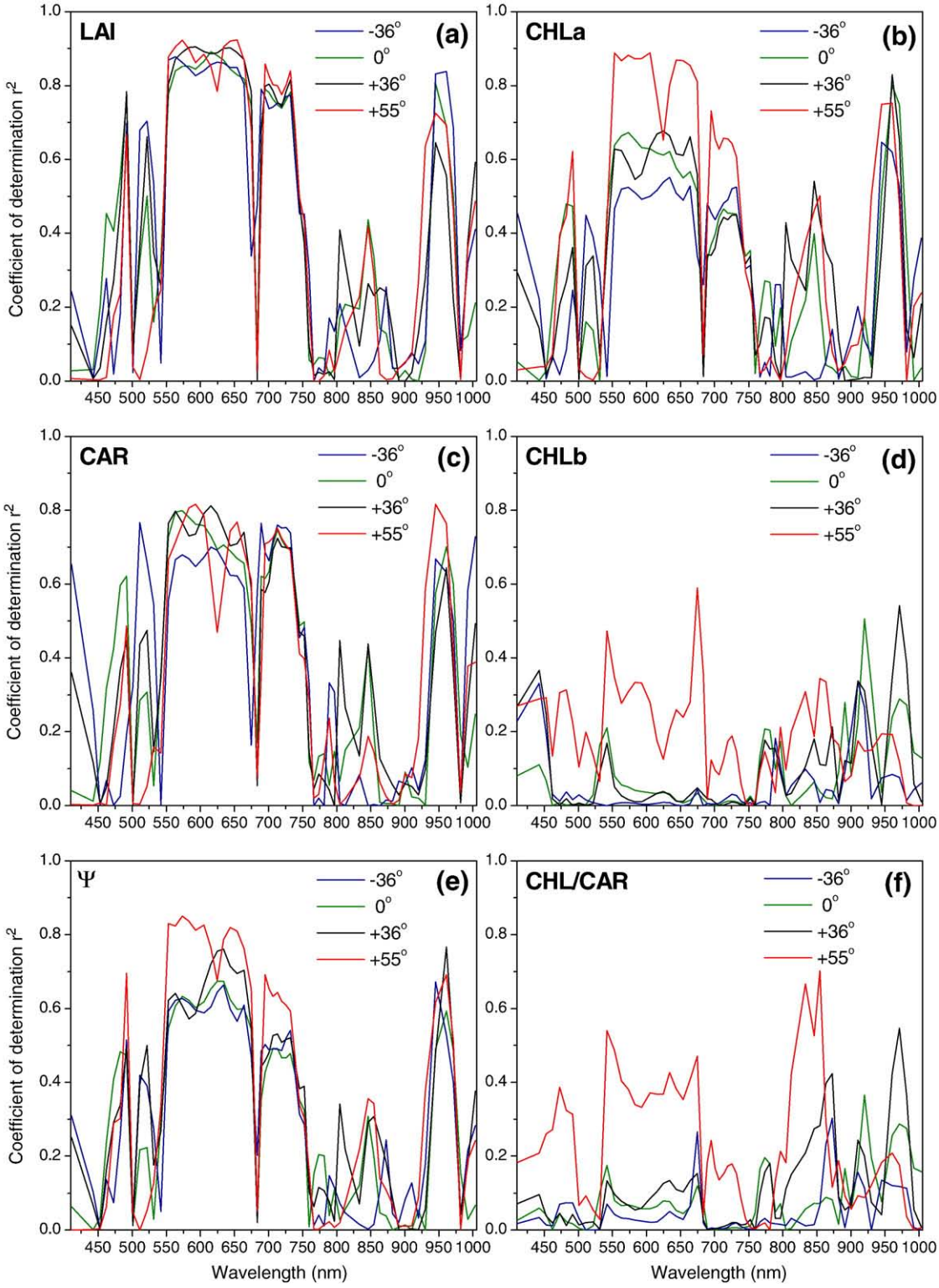

Fig. 5. Coefficients of determination (r^2) between CHRIS reflectance derivatives (D_x) and the ground measured biophysical and biochemical parameters for the four of the CHRIS observation angles.

NDSIs with extreme high significance ($r^2>0.9$), also implying that high observing angles may serve better for LAI estimation.

Contour maps of the other ecosystem variables (Fig. 6e–x) do not show regions of high significance as wide as LAI. Significance is found mostly in small wavelength regions or even in single band combinations. Starting with leaf chlorophyll content, it is rather strange how different is the variation of the significance between the +55° observing angle (Fig. 6e,i) and all the others (Fig. 6f–h, 6j–l). In CHLa determination (Fig. 6e–h), there is a relatively wide region of significant coefficients at NDSIs with *x*: ~620–710 nm and *y*: ~720–1003 nm at the +55° angle, whereas only smaller regions with significant coefficients may be found in the other observing angles. Accordingly, in CHLb determination (Fig. 6i–l), the +55° angle shows greater significance than the other angles. Although there is no NDSI

Table 4
Coefficients of determination (r^2) between published indices (Table 2) and the ground measured biophysical and biochemical parameters for the four of the CHRIS observation angles. Relationships that do not present statistical significance ($p>0.01$) are shaded. Among the statistically significant relationships, those with $r^2>0.7$ are highlighted in bold.

	LAI				CHLa				CHLb				CAR				CHL/CAR				Ψ			
	+55°	+36°	0°	-36°	+55°	+36°	0°	-36°	+55°	+36°	0°	-36°	+55°	+36°	0°	-36°	+55°	+36°	0°	-36°	+55°	+36°	0°	-36°
Broadband Greenness																								
EVI	**0.83**	**0.80**	**0.77**	**0.78**	0.67	0.42	0.46	0.50	0.15	0.00	0.01	0.02	**0.75**	0.70	**0.73**	**0.75**	0.16	0.01	0.00	0.01	0.65	0.53	0.48	0.52
Green NDVI	0.65	**0.72**	**0.74**	**0.72**	0.66	0.26	0.28	0.45	0.23	0.01	0.00	0.00	0.67	0.49	0.49	0.67	0.23	0.00	0.00	0.01	0.55	0.34	0.36	0.51
NDVI	**0.85**	**0.86**	**0.85**	**0.81**	**0.82**	0.43	0.46	0.53	0.26	0.00	0.01	0.01	**0.78**	0.66	0.66	**0.72**	0.30	0.02	0.01	0.02	**0.75**	0.52	0.52	0.60
SR	**0.75**	**0.73**	**0.73**	**0.72**	0.65	0.34	0.36	0.47	0.17	0.00	0.00	0.01	**0.79**	0.62	0.64	**0.75**	0.14	0.00	0.00	0.00	0.59	0.39	0.39	0.51
Narrowband Greenness																								
CARI	0.36	0.65	0.57	0.00	0.62	0.42	0.40	0.01	0.61	0.05	0.06	0.04	0.38	0.43	0.27	0.05	0.50	0.13	0.20	0.02	0.45	0.33	0.41	0.01
GI	**0.91**	**0.87**	**0.81**	**0.83**	**0.76**	0.53	0.54	0.57	0.20	0.01	0.02	0.02	**0.79**	**0.77**	**0.79**	**0.78**	0.22	0.04	0.01	0.02	**0.75**	0.59	0.54	0.61
GVI	**0.91**	**0.90**	**0.84**	**0.85**	**0.78**	0.58	0.59	0.60	0.22	0.01	0.03	0.03	**0.78**	**0.78**	**0.80**	**0.77**	0.25	0.06	0.03	0.04	**0.79**	0.65	0.59	0.65
mCAI	**0.84**	**0.83**	**0.80**	**0.79**	0.65	0.50	0.52	0.51	0.12	0.01	0.01	0.01	**0.72**	**0.74**	**0.75**	**0.74**	0.16	0.03	0.01	0.01	0.65	0.58	0.53	0.54
mCAI2	**0.88**	**0.85**	**0.84**	**0.82**	**0.75**	0.48	0.49	0.51	0.20	0.00	0.01	0.01	**0.76**	**0.72**	**0.71**	**0.73**	0.24	0.03	0.01	0.01	**0.71**	0.55	0.53	0.56
MCARI	**0.83**	**0.81**	**0.77**	**0.78**	0.68	0.41	0.41	0.46	0.09	0.00	0.00	0.00	0.69	0.68	0.69	**0.73**	0.21	0.01	0.00	0.00	0.65	0.49	0.43	0.50
MCARI/OSAVI	**0.70**	**0.81**	**0.84**	**0.85**	0.65	0.45	0.49	0.51	0.08	0.01	0.00	0.00	0.47	0.62	0.67	0.70	0.34	0.03	0.02	0.02	0.61	0.56	0.54	0.58
MCARI2	**0.85**	**0.82**	**0.80**	**0.80**	0.70	0.46	0.47	0.50	0.15	0.00	0.01	0.01	**0.76**	**0.71**	**0.72**	**0.75**	0.18	0.02	0.01	0.01	0.68	0.55	0.50	0.53
MCARI2/OSAVI	**0.83**	**0.82**	**0.82**	**0.86**	**0.70**	0.60	0.63	0.62	0.15	0.02	0.03	0.04	0.63	**0.72**	**0.75**	**0.75**	0.28	0.09	0.06	0.06	**0.71**	**0.74**	0.68	0.66
mNDVI	**0.82**	**0.87**	**0.83**	**0.89**	**0.87**	0.52	0.56	0.56	0.40	0.01	0.02	0.01	0.68	0.70	**0.74**	0.68	0.45	0.05	0.03	0.05	**0.80**	0.63	0.59	0.65
mNDVI2	**0.86**	**0.88**	**0.83**	**0.89**	**0.84**	0.62	0.66	0.62	0.40	0.04	0.06	0.03	**0.70**	**0.78**	**0.80**	**0.72**	0.40	0.08	0.06	0.07	**0.81**	**0.71**	0.67	**0.71**
MSAVI	**0.81**	**0.78**	**0.76**	**0.77**	0.65	0.40	0.41	0.50	0.13	0.00	0.00	0.01	**0.76**	0.67	0.68	**0.76**	0.15	0.01	0.00	0.01	0.63	0.49	0.44	0.52
mSR	**0.72**	**0.77**	0.63	**0.75**	0.68	0.41	0.41	0.41	0.38	0.00	0.01	0.00	0.67	**0.71**	**0.74**	0.69	0.24	0.01	0.00	0.00	0.67	0.47	0.40	0.43
mSR2	**0.85**	**0.85**	**0.79**	**0.85**	**0.77**	0.54	0.58	0.54	0.36	0.02	0.04	0.02	**0.73**	**0.77**	**0.81**	**0.72**	0.29	0.04	0.02	0.03	**0.76**	0.61	0.57	0.58
MTCI	0.23	0.01	0.03	0.12	0.11	0.22	0.09	0.00	0.08	0.56	0.54	0.25	0.24	0.13	0.03	0.01	0.00	0.25	0.17	0.07	0.21	0.16	0.04	0.00
mTVI	**0.85**	**0.82**	**0.80**	**0.80**	0.70	0.46	0.47	0.50	0.15	0.00	0.01	0.01	**0.76**	**0.71**	**0.72**	**0.75**	0.18	0.02	0.01	0.01	0.68	0.55	0.50	0.53
mTVI/OSAVI	**0.83**	**0.82**	**0.82**	**0.86**	**0.70**	0.60	0.63	0.62	0.15	0.02	0.03	0.04	0.63	**0.72**	**0.75**	**0.75**	0.28	0.09	0.06	0.06	**0.71**	**0.74**	0.68	0.66
NDVI	**0.86**	**0.86**	**0.86**	**0.82**	**0.82**	0.45	0.47	0.54	0.26	0.00	0.01	0.01	**0.77**	0.67	0.68	**0.72**	0.31	0.03	0.01	0.03	**0.76**	0.55	0.53	0.61
NDVI2	**0.88**	**0.88**	**0.86**	**0.85**	**0.79**	0.55	0.57	0.61	0.25	0.02	0.03	0.03	**0.78**	**0.75**	**0.74**	**0.77**	0.28	0.05	0.04	0.05	**0.76**	0.63	0.61	0.68
OSAVI	**0.86**	**0.84**	**0.82**	**0.81**	**0.75**	0.44	0.46	0.54	0.20	0.00	0.00	0.01	**0.78**	0.68	0.69	**0.75**	0.23	0.02	0.01	0.02	**0.71**	0.54	0.50	0.58
RDVI	**0.85**	**0.82**	**0.80**	**0.80**	**0.72**	0.43	0.44	0.52	0.17	0.00	0.00	0.01	**0.77**	0.68	0.69	**0.75**	0.20	0.01	0.00	0.01	0.69	0.53	0.48	0.55
REP	0.23	0.62	**0.79**	**0.71**	0.25	0.49	0.66	0.48	0.07	0.03	0.05	0.01	0.06	0.51	0.56	0.46	0.37	0.13	0.20	0.09	0.25	0.52	**0.78**	0.58
SIPI	**0.78**	**0.87**	**0.86**	**0.88**	**0.87**	0.60	0.66	0.65	0.34	0.01	0.04	0.03	0.57	0.67	0.70	0.62	0.57	0.11	0.11	0.14	**0.77**	**0.72**	**0.71**	**0.79**
SIPI2	**0.71**	**0.85**	**0.86**	**0.87**	**0.85**	0.56	0.63	0.64	0.40	0.01	0.03	0.03	0.51	0.62	0.66	0.58	0.63	0.11	0.10	0.16	0.70	0.70	0.69	**0.78**
SPVI	**0.82**	**0.79**	**0.76**	**0.77**	0.65	0.43	0.43	0.49	0.13	0.00	0.00	0.01	**0.74**	0.69	**0.70**	**0.74**	0.15	0.01	0.00	0.01	0.64	0.53	0.46	0.50
SR	**0.75**	**0.73**	**0.72**	**0.71**	0.66	0.34	0.36	0.47	0.19	0.00	0.00	0.01	**0.79**	0.62	0.64	**0.75**	0.14	0.00	0.00	0.00	0.60	0.39	0.38	0.50
SR1	**0.83**	**0.80**	**0.79**	**0.78**	0.69	0.41	0.44	0.53	0.19	0.00	0.01	0.01	**0.80**	0.68	0.69	**0.77**	0.17	0.01	0.00	0.01	0.65	0.47	0.47	0.57
SR2	**0.80**	**0.76**	**0.75**	**0.74**	0.67	0.36	0.38	0.49	0.17	0.00	0.00	0.01	**0.80**	0.64	0.66	**0.75**	0.15	0.00	0.00	0.01	0.62	0.42	0.41	0.53
SR3	0.64	**0.70**	**0.72**	**0.71**	0.58	0.30	0.32	0.47	0.16	0.00	0.00	0.01	0.68	0.57	0.56	**0.73**	0.14	0.00	0.00	0.00	0.51	0.36	0.38	0.52
SR4	**0.89**	**0.91**	**0.86**	**0.87**	**0.78**	0.62	0.63	0.62	0.21	0.02	0.03	0.03	**0.73**	**0.79**	**0.80**	**0.76**	0.28	0.08	0.05	0.05	**0.81**	0.70	0.64	0.69
TCARI	**0.86**	**0.86**	**0.84**	**0.84**	**0.73**	0.48	0.49	0.49	0.12	0.00	0.00	0.00	0.67	0.70	**0.72**	**0.73**	0.27	0.02	0.01	0.01	**0.71**	0.58	0.52	0.54
TCARI/OSAVI	0.66	**0.79**	**0.84**	**0.90**	0.65	0.51	0.57	0.55	0.11	0.00	0.00	0.01	0.39	0.59	0.64	0.66	0.44	0.07	0.06	0.04	0.61	0.63	0.64	0.64
TSAVI	**0.86**	**0.83**	**0.82**	**0.80**	**0.75**	0.42	0.45	0.53	0.19	0.00	0.00	0.02	0.79	0.67	0.68	0.76	0.22	0.01	0.01	0.02	**0.71**	0.53	0.50	0.57
TVI	**0.85**	**0.83**	**0.81**	**0.79**	0.66	0.48	0.50	0.50	0.12	0.00	0.01	0.01	**0.72**	**0.73**	**0.74**	**0.74**	0.17	0.02	0.01	0.01	0.66	0.57	0.52	0.53
TVI/OSAVI	**0.82**	**0.82**	**0.82**	**0.84**	0.65	0.68	0.71	0.64	0.12	0.04	0.06	0.05	0.57	**0.79**	**0.78**	**0.75**	0.26	0.12	0.10	0.07	0.70	**0.80**	**0.76**	0.68
VOG	**0.84**	**0.86**	**0.86**	**0.83**	**0.74**	0.47	0.50	0.60	0.30	0.02	0.02	0.04	**0.72**	0.68	0.68	**0.73**	0.28	0.04	0.03	0.06	0.68	0.54	0.54	0.65
VOG2	**0.77**	**0.73**	0.69	0.67	0.56	0.41	0.42	0.49	0.12	0.01	0.01	0.02	0.61	0.60	0.58	0.61	0.15	0.03	0.02	0.04	0.57	0.48	0.47	0.55
Leaf pigment (Carotenoids, Anthocyanins)																								
ARI	0.32	0.33	0.19	0.38	0.14	0.47	0.46	0.41	0.01	0.12	0.19	0.19	0.20	0.43	0.51	0.48	0.01	0.15	0.06	0.07	0.25	0.54	0.33	0.30
BGI	0.00	0.19	0.05	0.12	0.02	0.02	0.03	0.10	0.11	0.04	0.14	0.00	0.01	0.10	0.01	0.30	0.11	0.02	0.04	0.04	0.01	0.01	0.00	0.08
BRI	0.48	0.56	0.51	**0.70**	0.50	0.55	0.61	0.40	0.32	0.08	0.12	0.03	0.34	0.58	**0.73**	0.34	0.30	0.13	0.06	0.13	0.49	0.65	0.50	0.50
CRI	0.11	0.45	0.53	0.26	0.14	0.12	0.09	0.18	0.04	0.02	0.05	0.01	0.17	0.27	0.21	0.30	0.04	0.00	0.01	0.00	0.14	0.14	0.19	0.24
CRI2	0.00	0.17	0.21	0.03	0.01	0.00	0.00	0.01	0.01	0.07	0.15	0.07	0.01	0.06	0.01	0.02	0.01	0.03	0.03	0.02	0.00	0.01	0.02	0.03
Red/Green	**0.88**	**0.91**	**0.86**	**0.87**	**0.77**	0.61	0.64	0.61	0.21	0.02	0.04	0.03	**0.74**	**0.79**	**0.81**	**0.76**	0.27	0.07	0.05	0.05	**0.81**	0.69	0.64	0.69
RGI	**0.90**	**0.92**	**0.86**	**0.87**	**0.79**	0.64	0.65	0.64	0.24	0.03	0.04	0.04	**0.75**	**0.79**	**0.80**	**0.76**	0.28	0.09	0.06	0.07	**0.82**	**0.72**	0.66	**0.72**
Stress																								
CI	0.57	0.66	0.59	0.62	0.58	0.38	0.32	0.46	0.19	0.00	0.00	0.02	0.50	0.62	0.57	0.66	0.25	0.01	0.00	0.02	0.49	0.42	0.32	0.48
DI	0.44	0.64	0.56	0.31	0.31	0.57	0.53	0.61	0.33	0.24	0.30	0.47	0.22	0.50	0.41	0.26	0.24	0.29	0.27	0.64	0.29	0.50	0.48	0.57
DPR2	0.05	0.63	0.60	0.41	0.05	0.52	0.37	0.62	0.15	0.14	0.02	0.24	0.02	0.41	0.23	0.24	0.10	0.30	0.20	0.65	0.04	0.46	0.42	0.66
DREP	**0.83**	**0.77**	**0.75**	**0.76**	0.67	0.44	0.46	0.49	0.16	0.01	0.01	0.02	**0.75**	**0.71**	**0.73**	**0.75**	0.17	0.01	0.00	0.01	0.66	0.53	0.48	0.49
LIC	0.18	0.39	0.42	0.46	0.29	0.38	0.50	0.15	0.38	0.03	0.08	0.00	0.12	0.38	0.65	0.12	0.30	0.09	0.03	0.06	0.26	0.51	0.39	0.22
NPCI	0.15	0.51	0.52	0.51	0.29	0.44	0.52	0.18	0.38	0.02	0.06	0.00	0.10	0.47	**0.70**	0.16	0.34	0.08	0.02	0.06	0.24	0.58	0.43	0.26
NPQI	0.16	0.45	0.26	0.02	0.31	0.23	0.11	0.18	0.23	0.01	0.01	0.10	0.10	0.46	0.12	0.21	0.43	0.00	0.02	0.02	0.10	0.20	0.17	0.12
PRI	**0.74**	**0.75**	**0.74**	**0.90**	0.63	0.68	0.73	0.60	0.19	0.09	0.14	0.05	0.54	**0.79**	**0.83**	0.66	0.26	0.12	0.09	0.09	0.66	0.70	0.60	0.69
PRI2	**0.85**	**0.87**	**0.83**	**0.92**	**0.74**	0.65	0.68	0.60	0.22	0.04	0.07	0.03	0.67	**0.82**	**0.84**	**0.72**	0.29	0.08	0.06	0.06	**0.77**	0.70	0.61	0.69
PSRI	**0.90**	**0.90**	**0.85**	**0.89**	**0.89**	0.66	0.70	0.67	0.33	0.04	0.06	0.05	**0.71**	**0.79**	**0.79**	**0.72**	0.44	0.11	0.09	0.11	**0.84**	**0.75**	**0.70**	**0.77**
SR5	0.32	0.00	0.23	0.34	0.29	0.02	0.03	0.11	0.41	0.15	0.05	0.06	0.27	0.01	0.20	0.40	0.12	0.18	0.09	0.10	0.29	0.02	0.03	0.13
SR6	**0.85**	**0.83**	0.58	0.59	**0.77**	0.64	0.44	0.62	0.35	0.06	0.02	0.12	**0.71**	**0.72**	0.56	0.53	0.29	0.14	0.04	0.21	**0.71**	**0.71**	0.45	0.61
SRPI	0.20	0.46	0.46	0.53	0.31	0.43	0.51	0.18	0.39	0.03	0.07	0.00	0.14	0.46	0.69	0.18	0.32	0.08	0.02	0.04	0.28	0.55	0.41	0.25
Water																								
fWBI	0.50	0.19	0.22	0.23	0.46	0.04	0.06	0.04	0.16	0.14	0.08	0.11	0.63	0.28	0.27	0.20	0.08	0.14	0.10	0.08	0.33	0.08	0.06	0.04
WI	**0.81**	0.66	**0.74**	**0.81**	**0.77**	0.38	0.46	0.58	0.22	0.00	0.01	0.02	**0.83**	0.55	0.65	0.69	0.20	0.02	0.02	0.07	0.65	0.51	0.48	0.61

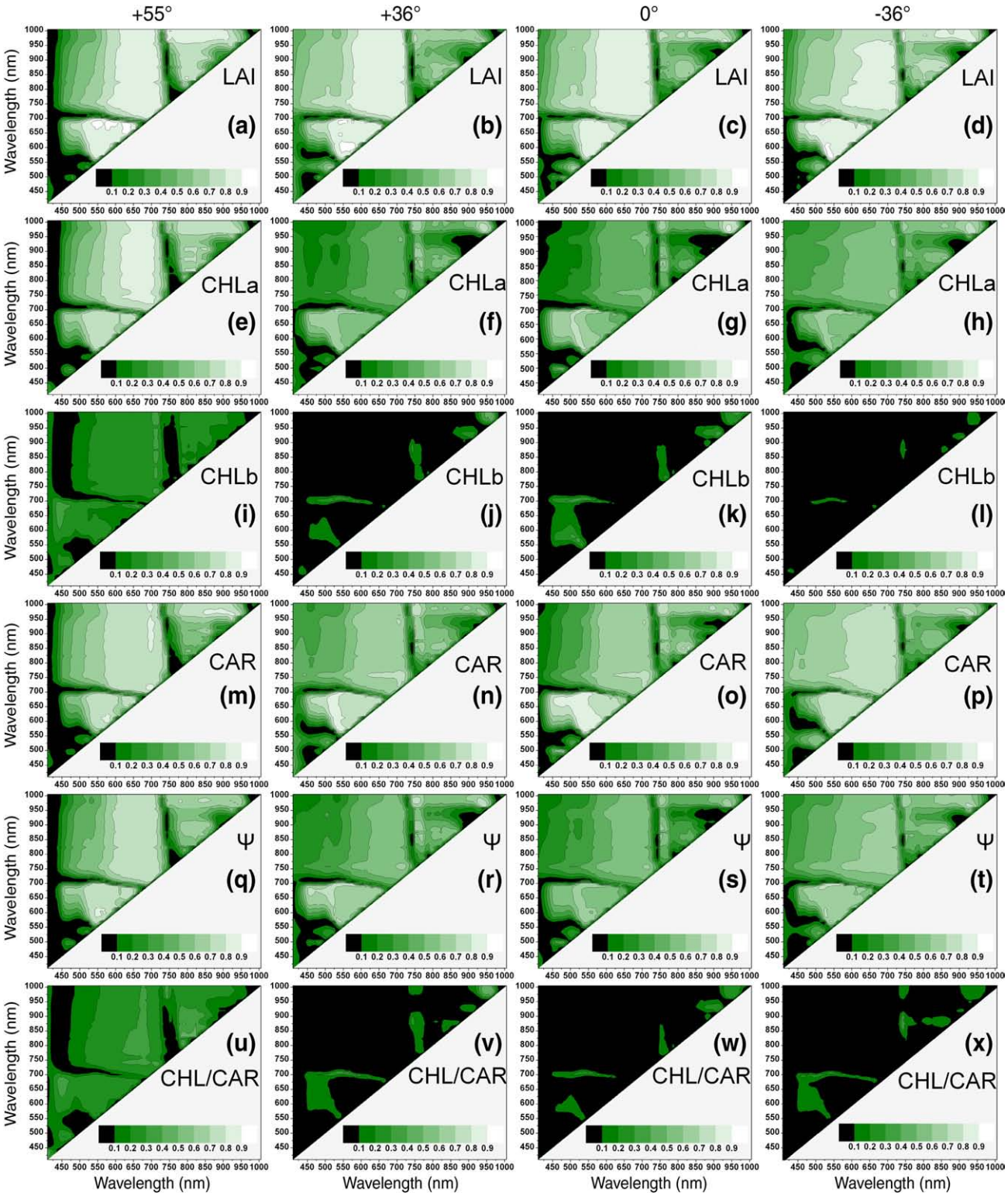

Fig. 6. Contour maps of coefficients of determination (r^2) between Normalized Difference Spectral Indices ($NDSI_{(x,y)}$, x and y are the wavelengths on the corresponding axes) and the ground measured biophysical and biochemical parameters for the four of the CHRIS observation angles (shown on top of the graph).

that correlate strongly (r^2>0.70) with CHLb (Table 5), the red-edge between 701 and 713 nm and NDSIs near $NDSI_{(532,553)}$ may contribute in CHLb determination.

CAR significance curves (Fig. 6m–p) follow the general outline of LAI and CHLa patterns. However, in contrast to CHLa, red-NIR NDSIs show relatively wider significant regions for CAR in all observing angles, with the higher significance around the red edge (695–707 nm). The most interesting combinations, in the perspective of carotenoid discrimination from chlorophylls and LAI, lie in the visible part of the spectrum. At the +36° and zenith observing angles (Fig. 6n,o), high significance areas appear for NDSIs with *x*: ~510–550 nm and *y*: ~570–700 nm. However, in zenith direction there is another small region of NDSIs with *x*: ~450–510 nm and *y*: ~660–680 nm that shows high correlation with CAR. Since the

Table 5
The NDSIs and SSIs that showed maximum coefficients of determination (r^2) in linear relationships with the ground measured biophysical and biochemical parameters for the four of the CHRIS observation angles. *x*, *y* correspond to index wavelengths.

	+55°			+36°			0°			−36°		
	r^2	*x*	*y*	r^2	*x*	*y*	r^2	*x*	*y*	r^2	*x*	*y*
$NDSI_{(x,y)}$												
LAI	0.956	616	689	0.914	583	593	0.872	719	739	0.934	542	563
CHLa	0.831	689	930	0.804	945	971	0.842	945	971	0.751	930	971
CHLb	0.552	664	683	0.524	961	982	0.430	532	707	0.283	664	683
CHL	0.801	689	930	0.805	961	971	0.820	961	971	0.698	945	961
CAR	0.830	701	713	0.845	522	634	0.862	511	675	0.792	593	616
CHL/CAR	0.484	789	833	0.534	961	982	0.341	616	695	0.398	616	695
Ψ	0.803	553	593	0.813	563	701	0.712	553	701	0.760	553	701
$SSI_{(x,y)}$												
LAI	0.935	605	689	0.921	574	695	0.891	605	625	0.888	553	563
CHLa	0.961	522	701	0.912	593	701	0.807	961	971	0.658	930	971
CHLb	0.794	501	707	0.736	616	701	0.503	910	930	0.371	910	920
CHL	0.963	511	701	0.908	605	701	0.784	961	971	0.601	930	971
CAR	0.837	920	971	0.814	605	625	0.805	563	574	0.773	491	522
CHL/CAR	0.744	812	864	0.899	616	701	0.709	616	701	0.307	625	695
Ψ	0.881	542	701	0.798	593	701	0.744	574	701	0.675	625	634

area 450–510 nm corresponds to carotenoid absorption wavelengths (Lichtenthaler, 1987), these indices may be especially suitable for carotenoid estimation.

Even though small high significance areas around the water absorption bands are evident for Ψ, the contour plots (Fig. 6q–t) reveal patterns similar to the ones for LAI and chlorophyll content. This may be explained by the high covariance between these variables (Fig. 2).

The contour maps for CHL/CAR (Fig. 6u–x) appear almost similar patterns with CHLb (Fig. 6i–l). The +55° observing angle gives wider significance areas compared to the other angles, while no angle shows strong correlations (Table 5).

3.6. Analysis of the $SSI_{(x,y)}$ formula experimental combinations

SSI combinations were calculated, analysed and tested in the same philosophy as the NDSIs. As shown in Fig. 7, zenith and especially −36° observing angles show the lower coefficients of determination (r^2) for all parameters compared to the forward scattering directions. Regarding LAI determinants (Fig. 7a–d), the red-NIR region does not seem so effective in the SSI formula as in NDSIs. However, the SSIs in the red–green region show very high coefficients of determination (r^2>0.9) in the forward scattering directions (Fig. 7a,b). In these directions, there is a common region of SSIs with *x*: ~540–620 nm and *y*: ~590–695 nm that reaches high significance, suggesting that a broadband NDVI (Table 2) may be replaced by a broadband $SSI_{(green,red)}$ for a more accurate LAI estimation, when forward scattering observing angle is available. Maximum r^2 in the forward scattering directions appears in indices based on the difference of green or yellow bands with red bands that are close to maximum chlorophyll absorbance (Table 5).

Similar to the patterns of NDSIs for chlorophyll content (Fig. 7e–l), the +55° SSIs (Fig. 7e,i) show higher coefficients than the rest of the available observing angles (Fig. 7f–h,j–l). In CHLa determination, high significance appears in the red–green, red–blue and the NIR water absorption wavelengths. Moreover, extreme high significance (r^2>0.9) appears at +55° SSIs with *x*: ~450–640 nm and *y*: ~570–705 nm (Fig. 7e). This wide region does not appear in the rest of the observing angles, where only smaller regions appear significant, located mainly in the lower wavelengths of the red edge region and the water absorption NIR (Fig. 7f–h). Interestingly, there is a common part, centred near 701 nm that is very important, predominating in both CHLa and CHLb determination for the forward scattering observing angles (Table 5).

CHLb determinants show lower significance than CHLa as described also in NDSI analysis (Table 5). However, in the SSI analysis there are some significant combinations in the forward scattering directions, combining a red edge band (701–713 nm) with a band at the blue–green–yellow region (Fig. 7i,j). As shown in Table 5, the best indices for total chlorophyll estimation, at least in the SSI analysis, are similar to the CHLa and the CHLb best indices.

CAR and Ψ contour plots (Fig. 7m–t) show similar results as in NDSI analysis, following the patterns of LAI and chlorophyll content. Concerning CAR determination, it is worth to note the highly significant SSIs based on blue wavelengths (491–552 nm) from the −36° observing angle (Fig. 7p), coinciding with the spectral region of carotenoid absorption.

Finally, CHL/CAR SSI determination patterns (Fig. 7u–x) resemble the CHLb patterns, as noticed also in the NDSI analysis. In the +55° angle, a significant region appears around $SSI_{(812,864)}$, resembling the peak in the derivative analysis (Fig. 5f). Additionally, significant areas appear in the red edge (701–713 nm) and – most importantly – around $SSI_{(616,701)}$ (Fig. 7v,w).

4. Discussion

In this study various aspects of satellite hyperspectral/multi-angular imagery for monitoring foliar biophysical and biochemical characteristics that are still under investigation were approached. Firstly, data were provided by an experimental satellite hyperspectral sensor (CHRIS) that is not widely used for ecological studies, especially in full spectral analysis (62 bands). Secondly, the capability of CHRIS to capture images from 5 different viewing angles with 1–2 min interval was used for vegetation index (VI) bi-directional analysis. Thirdly, the study of the effects that different vegetation parameters have on canopy reflectance spectrum was among the targets of this investigation. The spectral analysis and indices investigation revealed methods, CHRIS bands and simple but effective VIs for the estimation and discrimination of different ecosystem parameters. Lastly, the applicability of many published indices, with supposedly improved performance at the canopy scale, was tested on actual satellite hyperspectral measurements.

Viewing and illumination geometry significantly affect the reflectance spectra. Backward scattering observations originate mostly by sunlit leaves or branches (higher reflectance values), while forward scattering observations contain more signal from shaded leaves/branches and less from sunlit leaves (lower reflectance values). The fraction of sunlit leaves in forward scattering viewing

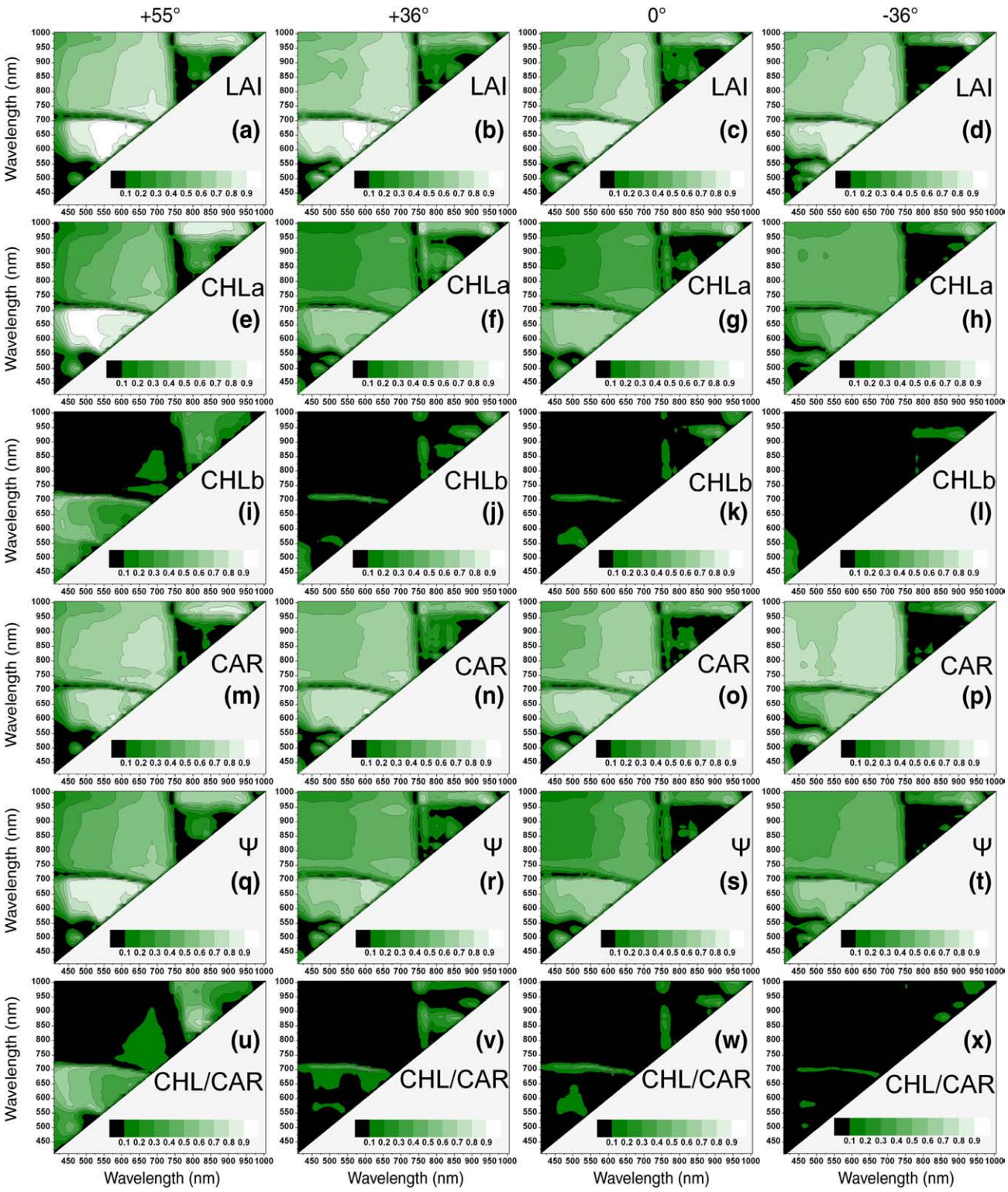

Fig. 7. Contour maps of coefficients of determination (r^2) between Simple Subtraction Indices ($SSI_{(x,y)}$, x and y are the wavelengths on the corresponding axes) and the ground measured biophysical and biochemical parameters for the four of the CHRIS observation angles (shown on top of the graph).

directions depends also on sun height. In addition to shadowing, gap fraction is another basic element of reflectance alteration. Nadir observation is highly affected by canopy gaps, depending mostly on the ecosystem type. Generally, the higher the observing angle is, the less canopy gaps the image contains. Canopy gap fraction decreases the quality and often the reflectance values of the signal. The above mechanisms are described also by Deering et al. (1999) and Sandmeier et al. (1998).

Studies that focus on the effects that view angle may have on reflectance often conclude that off-nadir observations are more useful in monitoring ecosystem physiology, since less background is visible within the field of view (Takebe et al., 1990). Moreover, it is often stated that back scattering directions serve better than forward scattering directions in the estimation of ecosystem biophysical parameters (Galvão et al., 2009; Walter-Shea et al., 1997). However, in our results the forward scattering observation angle (+55°) stands

out for the high coefficients of determination (r^2) in all the analysis sections. Although this angle is affected by shadowing, it is the highest zenith angle that is used in our analysis, with the lowest gap fraction included in the field of view. Thus, in the studied ecosystem, +55° images contain more foliar information while background effects are minimized. Our results imply that soil background influences are far more important than shadow effects regarding the reliability of the reflectance signal. Huber et al. (2007) also observed that CHRIS +55° angle performed similar to −55° in foliar nitrogen concentration prediction. Lastly, Verrelst et al. (2008) reported significant reflectance anisotropy of vegetation canopies and variable angular response of VIs and it was concluded that shadowing is not the prime-driving factor, but the proportion of photosynthetic, non-photosynthetic and background compounds significantly affects VI values.

The five analyses applied in this study aimed to reveal the attributes of the multiangular reflectance signal and its potential to estimate basic ecosystem parameters. Ideally, different parts of the spectrum would be sensitive to different ecosystem parameters, according to their spectral attributes. However, the use of 62 bands and all their NDSI and SSI combinations (resulting in 1891 VIs for each index type) may lead to misleading results. Except for the desired true relationships between VIs and plant parameters, cases of relationships due to parameter covariance or significant relationships may also appear by chance. Additionally, indirect reflectance responses to biochemical constituents may play a role in such relationships. For example, Haboudane et al. (2004) reported that chlorophyll concentration affects indirectly the reflectance curve even in infrared wavelengths, while Filella and Peñuelas (1994) stated that vegetation water content affects the reflectance indirectly at the red-edge region. The secondary effects of water content on a wide region of leaf spectral reflectance have also been reported by Carter (1991).

LAI proved to be the ecosystem parameter that is most easily extracted from reflectance. Reflectance derivatives in the green–red region and VIs of numerous wavelength combinations proved to be effective for LAI estimation. Traditional VIs that combine red and IR wavelengths, VIs of red and green bands, even VIs that use water absorption bands showed high significance in LAI determination. The latter are assumed to be the effect of covariation between leaf biomass and canopy water content. The indices that use red and green bands seem to have a little higher performance than the traditional IR-red indices. Green bands seem to improve performance of LAI and chlorophyll indices when combined with red and NIR bands (Broge and Leblanc, 2001; Gitelson et al., 1996), although indices that use only red and green bands are not often used for prediction of LAI. Many of the narrowband greenness indices (Table 2) tested in this study are designed to improve linearity and maximize sensitivity to biophysical parameters. For example, in the estimation of LAI by VIs, many studies have proven that several indices saturate at LAI values greater than 3 or 4 (Wang et al., 2005) and others have focused on the improvement of such indices (Haboudane et al., 2004). Our study is not ideal for extracting safe results about indices linearity to LAI, since the studied ecosystem reaches maximum LAI value about 3. In this view, it is reasonable that the traditional simple and improved indices performed similarly. Another aspect is the background effect on VIs. Indices like TCARI, MCARI, OSAVI and combinations of them, such as TCARI/OSAVI and MCARI/OSAVI, have been designed and tested to minimize background effects on predicting biophysical variables (Haboudane et al., 2002; Zarco-Tejada et al., 2005). However, in our results, even though the above indices provided significant relationships with LAI and chlorophyll content, they did not show improved performance compared to simpler ones, especially in the zenith direction, where canopy gaps are more obvious. The best LAI determinant proved to be $NDSI_{(616,689)}$ +55° (Table 6, Fig. 8a), with the combination of two close red hyperspectral bands performing better than NDVI.

Leaf chlorophyll content estimation required more attention and detailed overview of the analysis results than LAI. It is believed that an index designed for a specific vegetation biochemical parameter should not use the maximum absorbance wavelengths of this parameter, but wavelengths near them, because the peak wavelengths saturate fast in the increasing parameter volume (Datt, 1998; Gitelson and Merzlyak, 1994; Sims and Gamon, 2002). Regarding chlorophyll content, Gitelson et al. (1996) concluded that maximum sensitivity of chlorophyll concentration appears in the reflectance from 520 to 630 nm and also near 700 nm. Sims and Gamon (2002) highlighted the correlation of leaf chlorophyll content with leaf reflectance at 705 nm and le Maire et al. (2008) found best correlations with chlorophyll at 705 nm in reflectance at leaf level and 710 nm at canopy level. In this study, it is also shown that near red-edge wavelengths may play key role in chlorophyll determination, i.e. 701 nm for CHLa and 707 nm for CHLb (Fig. 4d). Finally, $SSI_{(511,701)}$ +55° and $SSI_{(605,701)}$ +36° are concluded to be the best estimators of the leaf chlorophyll content (Fig. 8g,h). In earlier studies that have also proposed indices using 700–710 nm as best chlorophyll wavelengths, a near infrared reference band was usually used (Gamon and Surfus, 1999; Gitelson and Merzlyak, 1994; Zarco-Tejada et al., 2001). In our study though, the reference band varies from green to orange, in accordance with le Maire et al. (2008), where the difference of the reflectance between 705 nm and 505 nm had distinguishable performance in chlorophyll estimation at canopy level. However, in leaf chlorophyll content analyses there were also many odd results. Especially in derivative and NDSI analysis, it is obvious that the best determinants focus around water absorption bands (Tables 3 and 5) even though chlorophyll affects the reflectance in the visible and the red-edge part of the spectrum. Consequently, this significant relationship may be due to chlorophyll content–water content covariance, which is typical for the studied ecosystem (Kyparissis and Manetas, 1993; Kyparissis et al., 1995).

The estimation of carotenoid content from reflectance is more difficult than the estimation of chlorophyll because of the overlap between the chlorophyll and carotenoid absorption peaks in the blue region of the spectrum and because of the higher concentration of chlorophyll than carotenoid in most healthy leaves. There have been some attempts for carotenoid estimation from leaf reflectance (Datt, 1998; Gitelson et al., 2002) but these indices were proven not to be generalizable across species or other data sets (Blackburn, 1998). In

Table 6
Indices and observation angles (z) that showed maximum coefficients of determination (r^2) for the estimation of each ground measured biophysical and biochemical parameter excluding results due to covariation or chance for all index types. x, y correspond to index wavelengths. The best index type for each variable is highlighted in bold.

	Reflectance R_x			**Derivative D_x**			**$NDSI_{(x,y)}$**				**$SSI_{(x,y)}$**			
	r^2	x	z	r^2	x	z	r^2	x	y	z	r^2	x	y	z
LAI	0.849	675	0°	0.923	654	+55°	**0.956**	**616**	**689**	**+55°**	0.935	605	689	+55°
CHLa	0.860	689	+55°	0.889	605	+55°	0.831	689	930	+55°	**0.961**	**522**	**701**	**+55°**
CHLb	0.567	707	+55°	0.589	675	+55°	0.552	664	683	+55°	**0.794**	**501**	**707**	**+55°**
CHL	0.856	689	+55°	0.865	553	+55°	0.801	689	930	+55°	**0.963**	**511**	**701**	**+55°**
CAR	0.274	411	+36°	0.766	511	−36°	**0.862**	**511**	**675**	**0°**	0.805	563	574	0°
CHL/CAR	0.508	701	+55°	0.541	542	+55°	0.452	583	701	+36°	**0.899**	**616**	**701**	**+36°**
Ψ	0.388	930	+36°	0.766	961	+36°	**0.800**	**945**	**971**	**+36°**	0.776	945	971	+36°

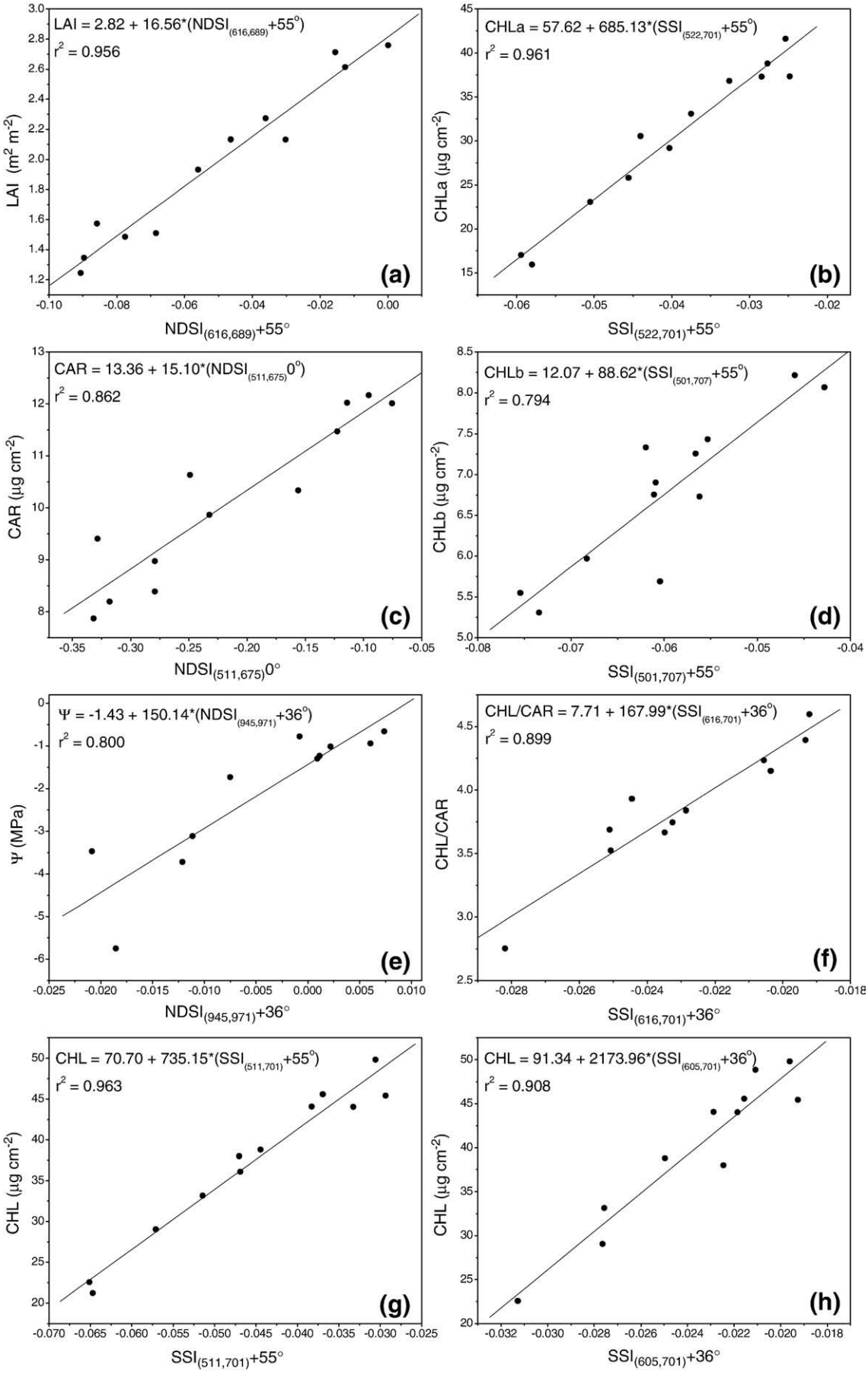

Fig. 8. Highlighted relationships (Table 6) between NDSIs/SSIs and the ground measured biophysical and biochemical parameters.

this study D_{411} and D_{511} were identified as potential indices, although it is concluded that $NDSI_{(511,675)}$ at 0° performed best in CAR determination (Fig. 8c). Gitelson et al. (2002) referred that the maximum sensitivity of reflectance to carotenoids occurs around 510 nm, where chlorophyll absorption ends and carotenoid absorption starts to decline. However, the proposed versions of CRI (Table 2) did not serve well in CAR estimation. CRI is designed in leaf level studies and uses reflectance at 550 or 700–710 nm (related to chlorophyll) to remove the chlorophyll effect from reflectance at 510 nm (sensitive to carotenoids). In the present study it seems more sufficient to use reflectance at 675 nm as a reference. Many significant relationships occurred also by chance in CAR analyses, such as $NDSI_{(701,713)}+55°$ (Table 5) with wavelengths far out from the carotenoid absorbance region. The significance of this index may be due to chance or it may be ascribed to the connection between carotenoid and chlorophyll content (Fig. 2). Furthermore, $SSI_{(920,971)}+55°$ (Table 5) may also be a result of the effect of water availability in leaf biochemical constitution.

Due to LAI–CHL–CAR co-variation it is very difficult to state whether an index is more biophysically or more biochemically dependent. Moreover, LAI and chlorophyll content have similar effects on canopy reflectance, particularly in the spectral region from the green (550 nm) to the red edge (750 nm). Considering the LAI significance areas in derivative, NDSI and SSI analyses, it seems to be rather difficult to find indices that are unaffected by LAI fluctuations, since LAI showed great regions of significance in all analyses. However, there are some indices right at the limits of LAI significant regions, that are the most important for accurate biochemical estimation. $D_{675}+55°$ shows $r^2=0.810$ in CHLa determination, while a perfectly clear peak with $r^2=0.589$ is evident for CHLb (Fig. 5d). As a result, r^2 for total CHL determination at 675 nm is 0.827, only slightly lower than maximum r^2 appearing at 553 nm (Table 3). However, the corresponding r^2 values for LAI determination at 553 and 675 nm are 0.878 and 0.683, indicating that the derivative at 675 nm is less sensitive to structural variations, probably making it a more effective chlorophyll index. An important notice in NDSI and SSI analyses, regarding the discrimination of the combined LAI-chlorophyll effect on the reflectance signal, is that the limits of the red–green significant region in LAI estimation (Figs. 6a–d, 7a–d) reach 695 nm, although in chlorophyll estimation (Figs. 6e–l, 7e–l) the significance reaches 701 nm in CHLa and expands to 713 nm in CHLb determination. Moreover, the NDSIs and SSIs that use these near red edge wavelengths seem to play major role in chlorophyll determination as they show high r^2. Lastly, from SSI analysis it is concluded that $SSI_{(511,701)}+55°$ and $SSI_{(605,701)}+36°$ are the best determinants of total chlorophyll content (Table 5). However, since the corresponding r^2 for LAI is 0.808 and 0.518, $SSI_{(605,701)}+36°$ may be considered a more accurate chlorophyll index. This observation lead to the hypothesis that the red-edge bands (centred mostly at 701 nm) may help in the design of an index that could estimate better the chlorophyll content and be less affected from canopy structural parameters (e.g. LAI). Since all these indices use wavelengths around the limits of the LAI significance area, it may be assumed that better indices for such discrimination would appear if better sensor spectral analysis would be available. Following the above perspective in carotenoid estimation, $NDSI_{(511,675)}0°$ seems to be effective enough for pure carotenoid estimation ($r^2=0.862$), since the coefficients of determination that this index shows for LAI and CHL are 0.729 and 0.645 respectively. Regarding the published indices, it is observed that VIs that combine red with blue bands, such as BRI and NPCI (Table 4), show relatively good correlations with CAR and medium covariation with LAI and CHL. Consequently, the above indices may serve better than PRI2 (Table 3) in carotenoid estimation.

CHL/CAR can be used for diagnosing the physiological state of plants (Balaguer et al., 2002; Kyparissis et al., 1995, 2000; Munné-Bosch and Alegre, 2000), thus a stress index can result from its analyses. Unlike the other examined parameters that show covariation with LAI and similar significance patterns between each other, the CHL/CAR ratio shows different significance patterns in all analyses. The fact that its patterns are – in most cases – similar with the ones for chlorophyll b may be due to that both variables are connected to total chlorophyll variations and plant health. Chlorophyll content alone has been used as an indicator of plant stress, vigour and growth (Carter, 1994; Lichtenthaler, 1998). Consequently, it seems reasonable to observe similarities in results between the analyses of CHL/CAR and CHL. Analyses revealed $SSI_{(616,701)}+36°$ (Fig. 8f) as a suitable stress index that is unaffected by structural variations, since its r^2 with LAI is very low (0.169). Additionally, $SSI_{(812,864)}+55°$ (Table 5) and $D_{855}+55°$ (Table 3) seem also significant for the determination of the ratio. The relationship between CHL/CAR and this IR part of the spectrum cannot be explained by absorbance curves or covariation between plant parameters and may be due to chance or indirect reflectance responses (Filella and Peñuelas, 1994; Haboudane et al., 2004).

Finally, it is often shown in the results that the significant indices for leaf water potential determination are actually linked to chlorophyll variations. Most of the indices that yield maximum r^2 values for Ψ in all of the analyses (Tables 3 and 5) resemble the indices of CHL (e.g. PSRI, $SSI_{(542,701)}+55°$). Similar results were observed in chlorophyll determination, where best indices incorporated IR wavelengths (e.g. $NDSI_{(961,971)}0°$, $NDSI_{(945,971)}0°$). It seems that the mutuality of the relationship between water and chlorophyll content is so intense in the studied ecosystem that chlorophyll indices and water indices may interchange. Although WI and fWBI do not present strong relationships with Ψ, $NDSI_{(961,971)}0°$ or $NDSI_{(945,971)}0°$ can serve better for water content estimation based on the above perspective. Moreover, $NDSI_{(945,971)}+36°$ (Fig. 8e) appeared to be the best water index when results due to covariation or chance are excluded (Table 6). The reason of WI poor performance may lie in the studied species physiology. Peñuelas et al. (1993) found that WI worked best in species that lose cell wall elasticity in response to drought stress. However, Grammatikopoulos (1999) has shown that *Phlomis fruticosa* is a species with remarkable tissue elasticity throughout the year.

5. Conclusions

The analyses of this study indicated the potential of hyperspectral data in efficient ecophysiology monitoring. It is demonstrated that broad bands are capable of LAI detection, although it seems that narrow bands in the visible part of the spectrum may lead to more accurate LAI estimations. However, for the detection and discrimination of leaf biochemical constituents, narrow bands are rather essential. In this case, it seems that the narrower the bands are, the more effectively indices are calculated.

Multiangular observations showed that high viewing angles produce more effective VIs than zenith observations. Although the applicability of high observation angles seems promising, there is a need of further and more extensive study on the response of the various VIs in changing viewing and illumination angles. Moreover, similar hyperspectral/multiangular applications and deeper analyses (e.g. non-linear relationships) in other ecosystem types, and particularly those with high LAI, are necessary in order to infer generalizable results.

According to the above, high spectral and spatial resolution satellite sensors with large swath width that would be capable of frequent global coverage would be an interesting advance in vegetation remote sensing. This kind of data would offer great possibilities for multiple applications and analyses that could expand the present capabilities of accurate ecosystem monitoring and improve our understanding of global vegetation state, processes, change and dynamics.

Acknowledgements

CHRIS/PROBA data were provided by the European Space Agency in the framework of the Cat-1 project "Study of Ecosystem Dynamics using CHRIS/PROBA Hyperspectral data — HypED" (ID 3792). Stavros Stagakis is a recipient of a graduate scholarship from the Academy of Athens. Special thanks to Dr. Efi Levizou for her valuable guidance and help in our field campaigns and for critically reading of the manuscript. Three anonymous reviewers are also acknowledged for their useful comments and suggestions.

References

Balaguer, L., Pugnaire, F. I., Martinez-Ferri, E., Armas, C., Valladares, F., & Manrique, E. (2002). Ecophysiological significance of chlorophyll loss and reduced photochemical efficiency under extreme aridity in *Stipa tenacissima* L. *Plant and Soil*, *240*, 343−352.

Bannari, A., Huete, A. R., Morin, D., & Zagolski, F. (1996). Effects of soil color and brightness on vegetation indexes. *International Journal of Remote Sensing*, *17*, 1885−1906.

Barnes, J. D., Balaguer, L., Manrique, E., Elvira, S., & Davison, A. W. (1992). A reappraisal of the use of DMSO for the extraction and determination of chlorophylls a and b in lichens and higher plants. *Environmental and Experimental Botany*, *32*, 85−100.

Blackburn, G. A. (1998). Quantifying chlorophylls and caroteniods at leaf and canopy scales: An evaluation of some hyperspectral approaches. *Remote Sensing of Environment*, *66*, 273−285.

Bréda, N. J. J. (2003). Ground-based measurements of leaf area index: a review of methods, instruments and current controversies. *Journal of Experimental Botany*, *54*, 2403−2417.

Broge, N. H., & Leblanc, E. (2001). Comparing prediction power and stability of broadband and hyperspectral vegetation indices for estimation of green leaf area index and canopy chlorophyll density. *Remote Sensing of Environment*, *76*, 156−172.

Campbell, G. S. (1986). Extinction coefficients for radiation in plant canopies calculated using an ellipsoidal inclination angle distribution. *Agricultural and Forest Meteorology*, *36*, 317−321.

Carter, G. A. (1991). Primary and secondary effects on water content on the spectral reflectance of leaves. *American Journal of Botany*, *78*, 916−924.

Carter, G. A. (1994). Ratios of leaf reflectances in narrow wavebands as indicators of plant stress. *International Journal of Remote Sensing*, *15*, 697−703.

Chen, J. M., Liu, J., Leblanc, S. G., Lacaze, R., & Roujean, J. L. (2003). Multi-angular optical remote sensing for assessing vegetation structure and carbon absorption. *Remote Sensing of Environment*, *84*, 516−525.

Dash, J., & Curran, P. J. (2004). The MERIS terrestrial chlorophyll index. *International Journal of Remote Sensing*, *25*, 5403−5413.

Datt, B. (1998). Remote sensing of chlorophyll a, chlorophyll b, chlorophyll a + b, and total carotenoid content in eucalyptus leaves. *Remote Sensing of Environment*, *66*, 111−121.

Daughtry, C. S. T., Walthall, C. L., Kim, M. S., de Colstoun, E. B., & McMurtrey, J. E. (2000). Estimating corn leaf chlorophyll concentration from leaf and canopy reflectance. *Remote Sensing of Environment*, *74*, 229−239.

Dawson, T. P., Curran, P. J., & Plummer, S. E. (1998). LIBERTY — Modeling the effects of leaf biochemical concentration on reflectance spectra. *Remote Sensing of Environment*, *65*, 50−60.

Deering, D. W., Eck, T. F., & Banerjee, B. (1999). Characterization of the reflectance anisotropy of three boreal forest canopies in spring–summer. *Remote Sensing of Environment*, *67*, 205−229.

Drolet, G. G., Huemmrich, K. F., Hall, F. G., Middleton, E. M., Black, T. A., Barr, A. G., & Margolis, H. A. (2005). A MODIS-derived photochemical reflectance index to detect inter-annual variations in the photosynthetic light-use efficiency of a boreal deciduous forest. *Remote Sensing of Environment*, *98*, 212−224.

Filella, I., & Peñuelas, J. (1994). The red edge position and shape as indicators of plant chlorophyll content, biomass and hydric status. *International Journal of Remote Sensing*, *15*, 1459−1470.

Filella, I., Amaro, T., Araus, J. L., & Peñuelas, J. (1996). Relationship between photosynthetic radiation-use efficiency of barley canopies and the photochemical reflectance index (PRI). *Physiologia Plantarum*, *96*, 211−216.

Galvão, L. S., Roberts, D. A., Formaggio, A. R., Numata, I., & Breunig, F. M. (2009). View angle effects on the discrimination of soybean varieties and on the relationships between vegetation indices and yield using off-nadir Hyperion data. *Remote Sensing of Environment*, *113*, 846−856.

Gamon, J. A., & Surfus, J. S. (1999). Assessing leaf pigment content and activity with a reflectometer. *New Phytologist*, *143*, 105−117.

Gamon, J. A., Serrano, L., & Surfus, J. S. (1997). The photochemical reflectance index: An optical indicator of photosynthetic radiation use efficiency across species, functional types, and nutrient levels. *Oecologia*, *112*, 492−501.

Gandia, S., Fernández, G., García, J. C., & Moreno, J. (2004). Retrieval of vegetation biophysical variables from CHRIS/PROBA data in the SPARC campaing. *ESA SP, vol. 578*. (pp. 40−48).

Gao, F., Schaaf, C. B., Strahler, A. H., Jin, Y., & Li, X. (2003). Detecting vegetation structure using a kernel-based BRDF model. *Remote Sensing of Environment*, *86*, 198−205.

Gitelson, A., & Merzlyak, M. N. (1994). Quantitative estimation of chlorophyll-a using reflectance spectra: Experiments with autumn chestnut and maple leaves. *Journal of Photochemistry and Photobiology B: Biology*, *22*, 247−252.

Gitelson, A. A., & Merzlyak, M. N. (1997). Remote estimation of chlorophyll content in higher plant leaves. *International Journal of Remote Sensing*, *18*, 2691−2697.

Gitelson, A. A., Kaufman, Y. J., & Merzlyak, M. N. (1996). Use of a green channel in remote sensing of global vegetation from EOS-MODIS. *Remote Sensing of Environment*, *58*, 289−298.

Gitelson, A. A., Merzlyak, M. N., & Chivkunova, O. B. (2001). Optical properties and nondestructive estimation of anthocyanin content in plant leaves. *Photochemistry and Photobiology*, *74*, 38−45.

Gitelson, A. A., Zur, Y., Chivkunova, O. B., & Merzlyak, M. N. (2002). Assessing carotenoid content in plant leaves with reflectance spectroscopy. *Photochemistry and Photobiology*, *75*, 272−281.

Gómez-Chova, L., Alonso, L., Guanter, L., Camps-Valls, G., Calpe, J., & Moreno, J. (2008). Correction of systematic spatial noise in push-broom hyperspectral sensors: application to CHRIS/PROBA images. *Applied Optics*, *47*, F46−F60.

Govaerts, Y. M., Verstraete, M. M., Pinty, B., & Gobron, N. (1999). Designing optimal spectral indices: A feasibility and proof of concept study. *International Journal of Remote Sensing*, *20*, 1853−1873.

Grammatikopoulos, G. (1999). Mechanisms for drought tolerance in two Mediterranean seasonal dimorphic shrubs. *Functional Plant Biology*, *26*, 587−593.

Grossman, Y. L., Ustin, S. L., Jacquemoud, S., Sanderson, E. W., Schmuck, G., & Verdebout, J. (1996). Critique of stepwise multiple linear regression for the extraction of leaf biochemistry information from leaf reflectance data. *Remote Sensing of Environment*, *56*, 182−193.

Guanter, L., Richter, R., & Moreno, J. (2006). Spectral calibration of hyperspectral imagery using atmospheric absorption features. *Applied Optics*, *45*, 2360−2370.

Guyot, G., Baret, F., & Major, D. J. (1988). High spectral resolution: Determination of spectral shifts between the red and near infrared. *International Archives of the Photogrammetry and Remote Sensing*, *27*, 750−760.

Haboudane, D., Miller, J. R., Tremblay, N., Zarco-Tejada, P. J., & Dextraze, L. (2002). Integrated narrow-band vegetation indices for prediction of crop chlorophyll content for application to precision agriculture. *Remote Sensing of Environment*, *81*, 416−426.

Haboudane, D., Miller, J. R., Pattey, E., Zarco-Tejada, P. J., & Strachan, I. B. (2004). Hyperspectral vegetation indices and novel algorithms for predicting green LAI of crop canopies: Modeling and validation in the context of precision agriculture. *Remote Sensing of Environment*, *90*, 337−352.

Horler, D. N. H., Dockray, M., & Barber, J. (1983). The red edge of plant leaf reflectance. *International Journal of Remote Sensing*, *4*, 273−288.

Huber, S., Kneubuehler, M., Koetz, B., Schopfer, J. T., Zimmermann, N. E., & Itten, K. I. (2007). The potential of spectrodirectional chris/proba data for biochemistry estimation. *ESA SP, vol. 636*. (pp. 6).

Huete, A. R., Jackson, R. D., & Post, D. F. (1985). Spectral response of a plant canopy with different soil backgrounds. *Remote Sensing of Environment*, *17*, 37−53.

Huete, A. R., Liu, H. Q., Batchily, K., & vanLeeuwen, W. (1997). A comparison of vegetation indices global set of TM images for EOS-MODIS. *Remote Sensing of Environment*, *59*, 440−451.

Jacquemoud, S., Ustin, S. L., Verdebout, J., Schmuck, G., Andreoli, G., & Hosgood, B. (1996). Estimating leaf biochemistry using the PROSPECT leaf optical properties model. *Remote Sensing of Environment*, *56*, 194−202.

Jones, H. G. (1992). *Plants and microclimate: A quantitative approach to environmnental plant physiology*. : Cambridge University Press.

Jordan, C. F. (1969). Derivation of leaf area index from quality of light on the forest floor. *Ecology*, *50*, 663−666.

Karnieli, A., Kaufman, Y. J., Remer, L., & Wald, A. (2001). AFRI — Aerosol free vegetation index. *Remote Sensing of Environment*, *77*, 10−21.

Kaufman, Y. J., & Tanre, D. (1992). Atmospherically Resistant Vegetation Index (Arvi) for Eos-Modis. *Ieee Transactions on Geoscience and Remote Sensing*, *30*, 261−270.

Kim, M. S., Daughtry, C. S. T., Chappelle, E. W., McMurtrey, J. E. III, & Walthall, C. L. (1994). The use of high spectral resolution bands for estimating absorbed photosynthetically active radiation (APAR). *6th symposium on physical measurements and signatures in remote sensing, Val D'Isere, France*.

Kimes, D. S., Newcomb, W. W., Tucker, C. J., Zonneveld, I. S., Vanwijngaarden, W., Deleeuw, J., & Epema, G. F. (1985). Directional reflectance factor distributions for cover types of northern Africa. *Remote Sensing of Environment*, *18*, 1−19.

Kyparissis, A., & Manetas, Y. (1993). Seasonal leaf dimorphism in a semi-deciduous Mediterranean shrub — Ecophysiological comparisons between winter and summer leaves. *Acta Oecologica—International Journal of Ecology*, *14*, 23−32.

Kyparissis, A., Petropoulou, Y., & Manetas, Y. (1995). Summer survival of leaves in a soft-leaved shrub (*Phlomis fruticosa* L, Labiatae) under Mediterranean field conditions: Avoidance of photoinhibitory damage through decreased chlorophyll contents. *Journal of Experimental Botany*, *46*, 1825−1831.

Kyparissis, A., Drilias, P., & Manetas, Y. (2000). Seasonal fluctuations in photoprotective (xanthophyll cycle) and photoselective (chlorophylls) capacity in eight Mediterranean plant species belonging to two different growth forms. *Australian Journal of Plant Physiology*, *27*, 265−272.

le Maire, G., François, C., Soudani, K., Berveiller, D., Pontailler, J. Y., Bréda, N., Genet, H., Davi, H., & Dufrêne, E. (2008). Calibration and validation of hyperspectral indices for the estimation of broadleaved forest leaf chlorophyll content, leaf mass per area, leaf area index and leaf canopy biomass. *Remote Sensing of Environment*, *112*, 3846−3864.

Lichtenthaler, H. K. (1987). Chlorophylls and carotenoids: Pigments of photosynthetic biomembranes. *Methods in Enzymology*, *148*, 350−382.

Lichtenthaler, H. K. (1998). The stress concept in plants: An introduction. *Stress of Life*, *851*, 187−198.
Lichtenthaler, H. K., & Wellburn, A. R. (1983). Determinations of total carotenoids and chlorophylls a and b of leaf extracts in different solvents. *Biochemical Society Transactions*, *11*, 591−592.
Lichtenthaler, H. K., Lang, M., Sowinska, M., Heisel, F., & Miehe, J. A. (1996). Detection of vegetation stress via a new high resolution fluorescence imaging system. *Journal of Plant Physiology*, *148*, 599−612.
Merzlyak, M. N., Gitelson, A. A., Chivkunova, O. B., & Rakitin, V. Y. (1999). Non-destructive optical detection of pigment changes during leaf senescence and fruit ripening. *Physiologia Plantarum*, *106*, 135−141.
Monsi, M., & Saeki, T. (1953). Uber den Lichtfaktor in den Pflanzengesellschaften und seine Bedeutung fur die Stoffproduktion. *Japanese Journal of Botany*, *14*, 22−52.
Munné-Bosch, S., & Alegre, L. (2000). Changes in carotenoids, tocopherols and diterpenes during drought and recovery, and the biological significance of chlorophyll loss in *Rosmarinus officinalis* plants. *Planta*, *210*, 925−931.
Norman, J. M., & Jarvis, P. G. (1974). Photosynthesis in Sitka Spruce (Picea-Sitchensis (Bong) Carr). 3. Measurements of canopy structure and interception of radiation. *Journal of Applied Ecology*, *11*, 375−398.
Oppelt, N., & Mauser, W. (2001). The chlorophyll content of maize (*Zea mays*) derived with the Airborne Imaging Spectrometer AVIS. *8th International Symposium "Physical Measurements and Signatures in Remote Sensing", Aussois, France* (pp. 407−412).
Peñuelas, J., Filella, I., Biel, C., Serrano, L., & Savé, R. (1993). The reflectance at the 950–970 Nm region as an indicator of plant water status. *International Journal of Remote Sensing*, *14*, 1887−1905.
Peñuelas, J., Gamon, J. A., Fredeen, A. L., Merino, J., & Field, C. B. (1994). Reflectance indices associated with physiological changes in nitrogen- and water-limited sunflower leaves. *Remote Sensing of Environment*, *48*, 135−146.
Peñuelas, J., Filella, I., Lloret, P., Munoz, F., & Vilajeliu, M. (1995). Reflectance assessment of mite effects on apple trees. *International Journal of Remote Sensing*, *16*, 2727−2733.
Qi, J., Chehbouni, A., Huete, A. R., Kerr, Y. H., & Sorooshian, S. (1994). A modified soil adjusted vegetation index. *Remote Sensing of Environment*, *48*, 119−126.
Qi, J., Moran, M. S., Cabot, F., & Dedieu, G. (1995). Normalization of sun/view angle effects using spectral Albedo-based vegetation indexes. *Remote Sensing of Environment*, *52*, 207−217.
Rondeaux, G., Steven, M., & Baret, F. (1996). Optimization of soil-adjusted vegetation indices. *Remote Sensing of Environment*, *55*, 95−107.
Roujean, J. L., & Breon, F. M. (1995). Estimating PAR absorbed by vegetation from bidirectional reflectance measurements. *Remote Sensing of Environment*, *51*, 375−384.
Sandmeier, S., Muller, C., Hosgood, B., & Andreoli, G. (1998). Physical mechanisms in hyperspectral BRDF data of grass and watercress. *Remote Sensing of Environment*, *66*, 222−233.
Sims, D. A., & Gamon, J. A. (2002). Relationships between leaf pigment content and spectral reflectance across a wide range of species, leaf structures and developmental stages. *Remote Sensing of Environment*, *81*, 337−354.
Takahashi, W., Nguyen-Cong, V., Kawaguchi, S., Minamiyama, M., & Ninomiya, S. (2000). Statistical models for prediction of dry weight and nitrogen accumulation based on visible and near-infrared hyper-spectral reflectance of rice canopies. *Plant Production Science*, *3*, 377−386.
Takebe, M., Yoneyama, T., Inada, K., & Murakami, T. (1990). Spectral reflectance ratio of rice canopy for estimating crop nitrogen status. *Plant and Soil*, *122*, 295−297.
Tucker, C. J. (1979). Red and photographic infrared linear combinations for monitoring vegetation. *Remote Sensing of Environment*, *8*, 127−150.
Verrelst, J., Schaepman, M. E., Koetz, B., & Kneubuhler, M. (2008). Angular sensitivity analysis of vegetation indices derived from CHRIS/PROBA data. *Remote Sensing of Environment*, *112*, 2341−2353.
Vincini, M., Frazzi, E., & D'Alessio, P. (2006). Angular dependence of maize and sugar beet Vis from directional CHRIS/PROBA data. *4th ESA CHRIS PROBA Workshop, ESRIN, Frascati, Italy* (pp. 19−21).
Vogelmann, J. E., Rock, B. N., & Moss, D. M. (1993). Red edge spectral measurements from sugar maple leaves. *International Journal of Remote Sensing*, *14*, 1563−1575.
Walter-Shea, E. A., Privette, J., Cornell, D., Mesarch, M. A., & Hays, C. J. (1997). Relations between directional spectral vegetation indices and leaf area and absorbed radiation in alfalfa. *Remote Sensing of Environment*, *61*, 162−177.
Wang, Q., Adiku, S., Tenhunen, J., & Granier, A. (2005). On the relationship of NDVI with leaf area index in a deciduous forest site. *Remote Sensing of Environment*, *94*, 244−255.
Zarco-Tejada, P. J., Miller, J. R., Noland, T. L., Mohammed, G. H., & Sampson, P. H. (2001). Scaling-up and model inversion methods with narrowband optical indices for chlorophyll content estimation in closed forest canopies with hyperspectral data. *Ieee Transactions on Geoscience and Remote Sensing*, *39*, 1491−1507.
Zarco-Tejada, P. J., Pushnik, J. C., Dobrowski, S., & Ustin, S. L. (2003). Steady-state chlorophyll a fluorescence detection from canopy derivative reflectance and double-peak red-edge effects. *Remote Sensing of Environment*, *84*, 283−294.
Zarco-Tejada, P. J., Berjón, A., López-Lozano, R., Miller, J. R., Martín, P., Cachorro, V., González, M. R., & de Frutos, A. (2005). Assessing vineyard condition with hyperspectral indices: Leaf and canopy reflectance simulation in a row-structured discontinuous canopy. *Remote Sensing of Environment*, *99*, 271−287.